

Tripartite quantum entanglement with squeezed optomechanics

Ya-Feng Jiao,^{1,2} Yun-Lan Zuo,³ Yan Wang,^{1,2} Wangjun Lu,⁴ Jie-Qiao Liao,³ Le-Man Kuang,^{2,3,*} and Hui Jing^{2,3,†}

¹*School of Electronics and Information, Zhengzhou University of Light Industry, Zhengzhou 450001, China*

²*Academy for Quantum Science and Technology, Zhengzhou University of Light Industry, Zhengzhou 450002, China*

³*Key Laboratory of Low-Dimensional Quantum Structures and Quantum Control of Ministry of Education,*

Department of Physics and Synergetic Innovation Center for Quantum Effects and Applications,

Hunan Normal University, Changsha 410081, China

⁴*Institute of Engineering Education and Engineering Culture Innovation and Department of Maths and Physics,*

Hunan Institute of Engineering, Xiangtan 411104, China

(Dated: August 7, 2024)

The ability to engineer entangled states that involve macroscopic objects is of particular importance for a wide variety of quantum-enabled technologies, ranging from quantum information processing to quantum sensing. Here we propose how to achieve coherent manipulation and enhancement of quantum entanglement in a hybrid optomechanical system, which consists of a Fabry-Pérot cavity with two movable mirrors, an optical parametric amplifier (OPA), and an injected squeezed vacuum reservoir. We show that the advantages of this system are twofold: (i) one can effectively regulate the light-mirror interactions by introducing a squeezed intracavity mode via the OPA; (ii) when properly matching the squeezing parameters between the squeezed cavity mode and the injected squeezed vacuum reservoir, the optical input noises can be suppressed completely. These peculiar features of this system allow us to generate and manipulate quantum entanglement in a coherent and controllable way. More importantly, we also find that such controllable entanglement, under some specific squeezing parameters, can be considerably enhanced in comparison with those of the conventional optomechanical system. Our work, providing a promising method to regulate and tailor the light-mirror interaction, are poised to serve as a useful tool for engineering various quantum effects which are based on cavity optomechanics.

I. INTRODUCTION

Entanglement, as a unique feature of quantum mechanics, is an appealing resource that enables a wide range of emerging quantum technologies [1]. For example, entangled resources have been required to implement complex calculations on quantum computers [2], to perform quantum communication tasks with security [3–5], and to circumvent the standard quantum limit for quantum sensing [6–8]. So far, a great deal of efforts have been devoted to generating, manipulating and storing entanglement from theories to experiments [9], which involve photons [10, 11], ions [12, 13], atomic ensembles [14–16], and superconducting circuits [17, 18]. Moreover, with the rapid advances on ground-state cooling of mechanical oscillators [19–21], the recent exploration of entanglement has also been extended to the domain of cavity optomechanics (COM) [22–24], achieving macroscopic entangled states between light and motion [25–29], between optical radiation fields [30–32], and between mechanical vibrations [33–39]. In very recent experiments, by exploiting the multi-tone driving field as an intermediary, direct observation of deterministic entanglement generation was even demonstrated between two massive mechanical oscillators with high fidelity [38, 39]. Beyond these classes of bipartite entanglement, quantum entanglement shared by more than two partitions can play a more essential role in the development of programmable quantum networks [40, 41] and controllable dense coding [42]. Recently, by integrating another degree of freedom to COM system, several promising schemes have also

been proposed theoretically for achieving full tripartite entanglement, which includes magnon-photon-phonon entanglement [43], atom-light-mirror entanglement [44], and light-mirror-mirror entanglement [45], to name a few. Nevertheless, due to the weak COM coupling strength and the typical rapid decoherence of mechanical oscillators, it still remains a tough challenge to prepare highly entangled states based on COM system. To avoid such difficulties, various theoretical approaches have been developed by exploiting synthetic gauge field [45, 46], reservoir engineering [47–49], dark-mode or feedback control [50–52], photon counting [53], dynamical modulation [54–56], and optical nonreciprocity [57–59].

In parallel, squeezed optical devices, which combine the techniques of OPA and reservoir engineering, open up a new route to enhance the light-matter interactions while suppress the input quantum noises, which boosts the achievement of a wealth of quantum phenomena. For example, several pioneering works on squeezed optical devices have contributed to the demonstration of photon blockade [60], entanglement between two atoms [61], long-lived or entangled cat states [62, 63], and optical squeezing beyond 3 dB limit [64]. Particularly, Lü *et al.* has predicted for the first time that by using a squeezed COM system, a single-photon quantum process can be observed even when the system is originally prepared in the weak COM coupling regime [60], which is owing to the exponential enhancement of the effective COM interaction in this system. Notably, such a strategy has also been utilized to realize nonreciprocal photon blockade [65–67] and nonreciprocal magnon laser [68] very recently. Besides, similar advances have also been achieved in making squeezed acoustic devices by employing quadratic COM coupling or mechanical parametric drive [69–71], which enables a variety of quantum effects, such as quantum phase transi-

* lmkuang@hunnu.edu.cn

† jinghui73@gmail.com

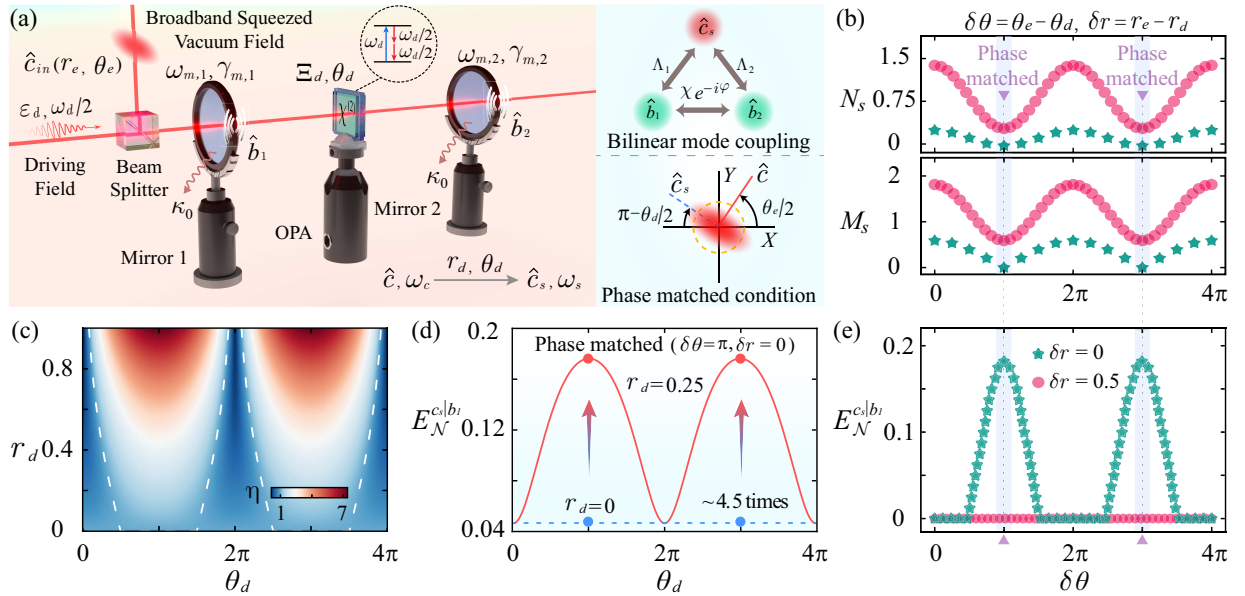


FIG. 1. Enhancing light-mirror interactions and simultaneously suppressing light-reservoir interaction in squeezed COM systems. (a) Schematic diagram and interaction picture of a squeezed COM system consisting of an FP cavity and a nonlinear $\chi^{(2)}$ medium. The driving fields of this system include a coherent pump laser with amplitude ε_d and frequency $\omega_d/2$, and a broadband squeezed laser with squeezing degree r_e and reference phase θ_e around central frequency ω_c . (b) The effective optical thermal noise N_s , the effective two-photon correlation strength M_s and (e) the logarithmic negativity $E_{\mathcal{N}}^{cs|b_l}$ versus the phase difference $\delta\theta$ for different values of δr . (c) Density plot of the enhancement factor η of the COM interaction as a function of the squeezing degree r_d and the squeezing reference angle θ_d . (d) The logarithmic negativity $E_{\mathcal{N}}^{cs|b_l}$ versus the squeezing reference angle θ_d under phase-matched condition achieving at $\delta r = 0$ and $\delta\theta = \pm n\pi$ ($n = 1, 3, 5, \dots$). The parameters are chosen as follows: $\omega_{m,j}/\omega_m = 1$, $\kappa/\omega_m = 0.9$, $\gamma_{m,j}/\omega_m = 10^{-5}$, $g_j/\omega_m = 0.2$, $\chi/\omega_m = 0.1$, $\bar{n}_{m,j} = 100$.

tion [72], quantum chaos [73], spin squeezing [74], photon blockade [75], and coherent state transfer [76]. However, as far as we know, the possibility of exploiting such powerful platform to create and manipulate highly entangled states with respect to massive mechanical oscillators, as well as protect the states from input noises, has not yet been reported up to now.

In this paper, we present how to achieve enhanced and controllable quantum entanglement by using a squeezed COM system. Here we consider a broadband squeezed laser field to be applied to a hybrid COM system consisting of a Fabry-Pérot (FP) cavity and an OPA, which we refer to as the squeezed COM system. We show that the interplay of the OPA and the squeezed laser field allows us to regulate the strength of both COM interaction and light-reservoir interaction simultaneously. This ability of the squeezed COM system plays a key role in the enhancement and manipulation of quantum entanglement. Interestingly, it is found that by tuning the squeezing parameters of the OPA, the degree of light-mirror, mirror-mirror and full tripartite entanglement, as well as the associated single-mode and two-mode quadrature squeezing, can be well regulated in a coherent and tunable way. Moreover, when further choosing proper squeezing parameters of the injected squeezed laser field to suppress the optical input noises, the COM entanglement, especially the tripartite one, can be considerably enhanced. Our proposal, providing a promising method to improve the performance of COM devices with multiple mechanical mirrors, can find its potential

applications in diverse areas, such as building phononic quantum network [3–5], synchronizing mechanical motions [77–79], and realizing dual-comb spectroscopy [80]. These findings will benefit not only for the exploration of macroscopic quantum phenomena, but also for the achievement of various entanglement-enabled quantum technologies, such as optomechanical quantum information processing [24, 81] and weak-force sensing [7, 8].

This paper is structured as follows. In Sec. II, we introduce the theoretical model of the squeezed COM system and derive the linearized Hamiltonian and the effective master equation of this system. In Sec. III, we first calculate the covariance matrix of this system and then evaluate the entanglement measures. Based on this numerical simulations, we explore the generation and manipulation of the light-mirror, mirror-mirror and full tripartite entanglement in this squeezed COM system. In Sec. IV, a summary is given.

II. THEORETICAL MODEL AND DYNAMICS OF A SQUEEZED COM SYSTEM

In this paper, we propose to generate, manipulate, and enhance quantum entanglement in a tunable and coherent way with a squeezed COM setup. As shown in Fig. 1(a), we consider a hybrid COM system consisting of an FP cavity and a nonlinear $\chi^{(2)}$ medium. The FP cavity supports one single optical mode with resonance frequency ω_c and two mechan-

ical vibrating modes with fundamental frequencies $\omega_{m,1}$ and $\omega_{m,2}$, respectively. The nonlinear $\chi^{(2)}$ medium can serve as an OPA that is pumped with frequency ω_d , amplitude Ξ_d , and phase θ_d . In a frame rotating with driving frequency $\omega_d/2$, the Hamiltonian of this system can be written as (setting $\hbar = 1$)

$$\begin{aligned} H &= H_c + H_m + H_{\text{om}} + H_{\text{dr}}, \\ H_c &= \Delta_c \hat{c}^\dagger \hat{c} + \Xi_d (e^{-i\theta_d} \hat{c}^{\dagger 2} + e^{i\theta_d} \hat{c}^2), \\ H_m &= \omega_{m,1} \hat{b}_1^\dagger \hat{b}_1 + \omega_{m,2} \hat{b}_2^\dagger \hat{b}_2 + \chi (e^{-i\varphi} \hat{b}_1^\dagger \hat{b}_2 + e^{i\varphi} \hat{b}_2^\dagger \hat{b}_1), \\ H_{\text{om}} &= -g_1 \hat{c}^\dagger \hat{c} (\hat{b}_1^\dagger + \hat{b}_1) - g_2 \hat{c}^\dagger \hat{c} (\hat{b}_2^\dagger + \hat{b}_2), \\ H_{\text{dr}} &= F_1 (\hat{b}_1^\dagger + \hat{b}_1) + F_2 (\hat{b}_2^\dagger + \hat{b}_2) + i\varepsilon_d (\hat{c}^\dagger - \hat{c}), \end{aligned} \quad (1)$$

where \hat{c} (\hat{c}^\dagger) and \hat{b}_j (\hat{b}_j^\dagger) are the annihilation (creation) operators of the cavity mode and the j th ($j = 1, 2$) mechanical mode, respectively, and $\Delta_c = \omega_c - \omega_d/2$ is the cavity-pump detuning. The first term H_c in Eq. (1) is the Hamiltonian of the cavity mode, in which the quadratic terms describe the nonlinear optical interaction induced by OPA. The second term H_m denotes the Hamiltonian of the mechanical mode, with χ the coupling strength of the phonon-hopping interaction and φ the corresponding modulation phase. The third term H_{om} describes Hamiltonian for the optical-radiation-pressure mediated interaction between the cavity mode and the two mechanical modes, and $g_j = (\omega_{c,j}/R_j) \sqrt{\hbar/m_j \omega_{m,j}}$ denotes the single-photon COM coupling strength, with R_j and m_j being the cavity length and the effective mass of the j th mechanical resonator, respectively. The last term H_{dr} is the Hamiltonian of the driving field, which includes two constant mechanical driving forces F_j and a coherent optical pump field. The constant mechanical driving forces F_j are applied to cancel the force induced by the parametric amplification (see detailed discussions below). The amplitude of the optical pump field is given by $|\varepsilon_d| = \sqrt{2\kappa P_d/\hbar\omega_d}$, where P_d is the input laser power and κ is the cavity decay rate.

In our proposed scheme, a broadband squeezed laser field \hat{c}_{in} , with squeezing degree r_e and reference phase θ_e around central frequency ω_c , is also introduced to act as the squeezed-vacuum reservoir that is linearly coupled to the FP cavity. For the two mechanical mirrors, they are assumed to be coupled with two independent thermal reservoirs at same bath temperature T . Considering such system-bath interactions for the optical and mechanical modes, the dynamics of the total system is governed by the following Born-Markovian master equation

$$\begin{aligned} \dot{\rho} &= i[\rho, H] + \frac{\kappa}{2}(N+1)\mathcal{D}[\hat{c}]\rho + \frac{\kappa}{2}N\mathcal{D}[\hat{c}^\dagger]\rho \\ &\quad - \frac{\kappa}{2}M\mathcal{G}[\hat{c}]\rho - \frac{\kappa}{2}M^*\mathcal{G}[\hat{c}^\dagger]\rho \\ &\quad + \sum_{j=1,2} \frac{\gamma_{m,j}}{2}(\bar{n}_{m,j}+1)\mathcal{D}[\hat{b}_j]\rho + \frac{\gamma_{m,j}}{2}\bar{n}_{m,j}\mathcal{D}[\hat{b}_j^\dagger]\rho, \end{aligned} \quad (2)$$

where

$$\begin{aligned} \mathcal{D}[\hat{o}]\rho &= 2\hat{o}\rho\hat{o}^\dagger - \hat{o}^\dagger\hat{o}\rho - \rho\hat{o}^\dagger\hat{o}, \\ \mathcal{G}[\hat{o}]\rho &= 2\hat{o}\rho\hat{o} - \hat{o}\hat{o}\rho - \rho\hat{o}\hat{o} \quad (\hat{o} = \hat{c}, \hat{b}_j), \end{aligned} \quad (3)$$

are the Lindblad operators, $[\cdot, \cdot]$ denotes the commutator, and $\gamma_{m,j}$ is the mechanical damping rate. $N = \sinh^2(r_e)$ and $M = \cosh(r_e) \sinh(r_e) e^{i\theta_e}$ describe the optical thermal noise and the strength of the two-photon correlation caused by the squeezed-vacuum reservoir, respectively. $\bar{n}_{m,j} = 1/[\exp(\omega_{m,j}/k_B T) - 1]$ represents the mean thermal phonon excitation number of the j th mechanical modes, with k_B the Boltzmann constant. Note that to obtain the master equation (2), we have assumed each mirror has a high quality factor, namely, $Q_{m,j} \equiv \omega_{m,j}/\gamma_{m,j} \gg 1$, which ensures that the system-bath interaction for the mechanical mode can be described by a Markovian process.

As discussed in detail in Ref. [60], the light-mirror interaction can be exponentially enhanced with the facility of the generation of squeezed cavity field enabled by OPA. Here, in order to introduce the squeezed cavity field in our system, one can perform the Bogoliubov transformation with a unitary operator, $S(\eta_d) = \exp[(-\eta_d \hat{c}^{\dagger 2} + \eta_d^* \hat{c}^2)/2]$, i.e.,

$$S^\dagger(\eta_d) \hat{c} S(\eta_d) = \cosh(r_d) \hat{c}_s - e^{-i\theta_d} \sinh(r_d) \hat{c}_s^\dagger, \quad (4)$$

where $\eta_d = r_d e^{-i\theta_d}$ is the complex squeezing parameter, with a squeezing strength $r_d = (1/4) \ln[(\Delta_c + 2\Xi_d)/(\Delta_c - 2\Xi_d)]$ and a squeezing reference angle θ_d . By applying the above Bogoliubov transformation and dropping the constant terms, the effective Hamiltonian of the total system is derived as

$$\begin{aligned} \tilde{H} &= \omega_s \hat{c}_s^\dagger \hat{c}_s + \omega_{m,1} \hat{b}_1^\dagger \hat{b}_1 + \omega_{m,2} \hat{b}_2^\dagger \hat{b}_2 + \chi (e^{-i\varphi} \hat{b}_1^\dagger \hat{b}_2 + e^{i\varphi} \hat{b}_2^\dagger \hat{b}_1) \\ &\quad - \zeta_{s,1} \hat{c}_s^\dagger \hat{c}_s (\hat{b}_1^\dagger + \hat{b}_1) + \frac{\zeta_{p,1}}{2} (e^{-i\theta_d} \hat{c}_s^{\dagger 2} + e^{i\theta_d} \hat{c}_s^2) (\hat{b}_1^\dagger + \hat{b}_1) \\ &\quad - \zeta_{s,2} \hat{c}_s^\dagger \hat{c}_s (\hat{b}_2^\dagger + \hat{b}_2) + \frac{\zeta_{p,2}}{2} (e^{-i\theta_d} \hat{c}_s^{\dagger 2} + e^{i\theta_d} \hat{c}_s^2) (\hat{b}_2^\dagger + \hat{b}_2) \\ &\quad + i\varepsilon_d \cosh(r_d) (\hat{c}_s^\dagger - \hat{c}_s) + i\varepsilon_d \sinh(r_d) (e^{-i\theta_d} \hat{c}_s^\dagger - e^{i\theta_d} \hat{c}_s). \end{aligned} \quad (5)$$

Here, $\omega_s = (\Delta_c - 2\Xi_d) \exp(2r_d)$ is referred to as the effective resonance frequency of the squeezed cavity mode, and we have chosen $F_j = g_j \sinh^2(r_d)$ to cancel the constant mechanical force induced by parametric amplification. Moreover, the effective COM coupling strength of the j th mechanical mode induced by the radiation pressure and the parametric amplification can be respectively expressed as

$$\begin{aligned} \zeta_{s,j} &= g_j \cosh(2r_d) = \frac{g_j \Delta_c}{\sqrt{\Delta_c^2 - 4\Xi_d^2}}, \\ \zeta_{p,j} &= g_j \sinh(2r_d) = \frac{2g_j \Xi_d}{\sqrt{\Delta_c^2 - 4\Xi_d^2}}. \end{aligned} \quad (6)$$

Correspondingly, the effective master equation under the Bogoliubov transformation can be derived as

$$\begin{aligned} \dot{\tilde{\rho}} &= i[\tilde{\rho}, \tilde{H}] + \frac{\kappa}{2}(N_s+1)\mathcal{D}[\hat{c}_s]\tilde{\rho} + \frac{\kappa}{2}N_s\mathcal{D}[\hat{c}_s^\dagger]\tilde{\rho} \\ &\quad - \frac{\kappa}{2}M_s\mathcal{G}[\hat{c}_s]\tilde{\rho} - \frac{\kappa}{2}M_s^*\mathcal{G}[\hat{c}_s^\dagger]\tilde{\rho} \\ &\quad + \sum_{j=1,2} \frac{\gamma_{m,j}}{2}(\bar{n}_{m,j}+1)\mathcal{D}[\hat{b}_j]\tilde{\rho} + \frac{\gamma_{m,j}}{2}\bar{n}_{m,j}\mathcal{D}[\hat{b}_j^\dagger]\tilde{\rho}, \end{aligned} \quad (7)$$

where

$$\begin{aligned} N_s &= \sinh^2(r_d) \cosh^2(r_e) + \cosh^2(r_d) \sinh^2(r_e) \\ &\quad + \frac{1}{2} \cos(\delta\theta) \sinh(2r_d) \sinh(2r_e), \\ M_s &= e^{i\theta_d} [\cosh(r_d) \cosh(r_e) + e^{-i\delta\theta} \sinh(r_d) \sinh(r_e)] \\ &\quad \times [\sinh(r_d) \cosh(r_e) + e^{i\delta\theta} \cosh(r_d) \sinh(r_e)] \end{aligned} \quad (8)$$

are the effective optical thermal noise and the effective two-photon correlation strength, respectively. Here $\delta\theta \equiv \theta_e - \theta_d$ is the phase difference between the squeezed intracavity field and the squeezed-vacuum reservoir, and $\tilde{\rho} = S^\dagger(\eta_d)\rho S(\eta_d)$ is an effective density operator of the total system. The detailed derivation process of the effective Hamiltonian (5) and the associated master equation (7) is reported in the Supporting Information. From Eq. (8), one can find that by choosing an equal squeezing strength of both the intracavity mode and the squeezed-vacuum reservoir, i.e., $r_d = r_e = r$, N_s and M_s can be simply reduced to

$$\begin{aligned} N_s &= \frac{1}{2} \sinh^2(2r)[1 + \cos(\delta\theta)], \\ M_s &= \frac{1}{2} e^{i\theta_d} \sinh(2r)(1 + e^{i\delta\theta})[\cosh^2(r) + e^{-i\delta\theta} \sinh^2(r)]. \end{aligned} \quad (9)$$

Equation (9) implies that when the phase-matched condition between the squeezed intracavity field and the squeezed-vacuum reservoir is fulfilled by setting $\delta r \equiv r_e - r_d = 0$ and $\delta\theta = \pm n\pi$ ($n = 1, 3, 5, \dots$), the effective optical thermal noise N_s and the effective two-photon-correlation strength M_s can thus be completely eliminated, that is, $N_s = M_s = 0$. In contrast, for other values of δr and $\delta\theta$, N_s and M_s cannot be reduced to zero, which is corresponding to the phase-mismatched regime. Figure 1(b) shows the dependence of the optical thermal noise N_s and the two-photon correlation strength M_s on the squeezing parameters δr and $\delta\theta$. This numerical result is consistent with the qualitative discussion, which is also reminiscent of those similar findings for squeezed quantum systems in the preceding studies [60–64]. These results mean that in the basis of the squeezed cavity field \hat{c}_s and under the phase-matched condition, i.e., $N_s = M_s = 0$, the squeezed-vacuum reservoir originally coupled to the cavity field \hat{c} becomes an effective vacuum reservoir [see Fig. 1(a) for more details]. Instead, for the phase-mismatched regime, the system will still be coupled to the squeezed-vacuum reservoir since the corresponding optical noise N_s and M_s is not equal to zero. Therefore, in order to enhance the COM coupling rate and simultaneously suppress the effective optical input noises, an essential procedure is to couple the system with a squeezed-vacuum reservoir and then properly choose the squeezing parameters to satisfy the phase-matched condition. Such squeezed COM systems with the phase-matched squeezed-vacuum reservoir have many advantages in the generation and manipulation of entanglement between light and mirrors, which will be further analyzed in the following discussions.

The Hamiltonian involved in master equation (7) includes the terms of nonlinear COM interactions between the optical

field and the mechanical mirrors. In this case, the dynamics of this system is difficult to be directly solved. In order to deal with this problem, one can linearize the Hamiltonian by expanding each operator as a sum of its steady-state mean value and a small quantum fluctuation around it under the condition of strong optical driving, i.e.,

$$\hat{c}_s = \bar{c}_s + \delta\hat{c}_s, \quad \hat{b}_j = \bar{b}_j + \delta\hat{b}_j. \quad (10)$$

By using the master equation (7), one can obtain the steady-state mean value of the optical field and the mechanical oscillators as

$$\begin{aligned} \bar{c}_s &= -\frac{(i\Delta_s - \frac{\kappa}{2})A_1 + iA_2\beta_p}{(\Delta_s^2 + \frac{\kappa^2}{4}) - \beta_p^2} \varepsilon_d, \\ \bar{b}_1 &= \frac{i\zeta_{s,1}|\bar{c}_s|^2 - i\frac{\zeta_{p,1}}{2}\alpha_s - i\chi e^{-i\varphi}\bar{b}_2}{i\omega_{m,1} + \frac{\gamma_{m,1}}{2}}, \\ \bar{b}_2 &= \frac{i\zeta_{s,2}|\bar{c}_s|^2 - i\frac{\zeta_{p,2}}{2}\alpha_s - i\chi e^{i\varphi}\bar{b}_1}{i\omega_{m,2} + \frac{\gamma_{m,2}}{2}}, \end{aligned} \quad (11)$$

with

$$\begin{aligned} \Delta_s &= \omega_s - \beta_s, \\ \alpha_s &= e^{-i\theta_d}\bar{c}_s^{*2} + e^{i\theta_d}\bar{c}_s^2, \\ \beta_s &= \zeta_{s,1}(\bar{b}_1^* + \bar{b}_1) + \zeta_{s,2}(\bar{b}_2^* + \bar{b}_2), \\ \beta_p &= \zeta_{p,1}(\bar{b}_1^* + \bar{b}_1) + \zeta_{p,2}(\bar{b}_2^* + \bar{b}_2), \\ A_1 &= \cosh(r_d) + \sinh(r_d)e^{-i\theta_d}, \\ A_2 &= \cosh(r_d)e^{-i\theta_d} + \sinh(r_d). \end{aligned} \quad (12)$$

Then, by using Eqs. (10) and (11), one can directly derive the linearized Hamiltonian and the associated master equation as

$$\begin{aligned} \tilde{H}_{lin} &= \Delta_s \hat{c}_s^\dagger \hat{c}_s + \omega_{m,1} \hat{b}_1^\dagger \hat{b}_1 + \omega_{m,2} \hat{b}_2^\dagger \hat{b}_2 \\ &\quad + \frac{1}{2} \beta_p (e^{-i\theta_d} \hat{c}_s^{\dagger 2} + e^{i\theta_d} \hat{c}_s^2) + \chi (e^{-i\varphi} \hat{b}_1^\dagger \hat{b}_2 + e^{i\varphi} \hat{b}_2^\dagger \hat{b}_1) \\ &\quad - (\Lambda_1 \hat{c}_s^\dagger + \Lambda_1^* \hat{c}_s)(\hat{b}_1^\dagger + \hat{b}_1) - (\Lambda_2 \hat{c}_s^\dagger + \Lambda_2^* \hat{c}_s)(\hat{b}_2^\dagger + \hat{b}_2), \end{aligned} \quad (13)$$

and

$$\begin{aligned} \dot{\tilde{\rho}} &= i[\tilde{\rho}, \tilde{H}_{lin}] + \frac{\kappa}{2}(N_s + 1)\mathcal{D}[\hat{c}_s]\tilde{\rho} + \frac{\kappa}{2}N_s\mathcal{D}[\hat{c}_s^\dagger]\tilde{\rho} \\ &\quad - \frac{\kappa}{2}M_s\mathcal{G}[\hat{c}_s]\tilde{\rho} - \frac{\kappa}{2}M_s^*\mathcal{G}[\hat{c}_s^\dagger]\tilde{\rho} \\ &\quad + \sum_{j=1,2} \frac{\gamma_{m,j}}{2}(\bar{n}_{m,j} + 1)\mathcal{D}[\hat{b}_j]\tilde{\rho} + \frac{\gamma_{m,j}}{2}\bar{n}_{m,j}\mathcal{D}[\hat{b}_j^\dagger]\tilde{\rho}, \end{aligned} \quad (14)$$

where

$$\Lambda_j = G_j \cosh(2r_d) - G_j^* \sinh(2r_d)e^{-i\theta_d} \quad (15)$$

is the effective COM coupling rate, with $G_j = g_j \bar{c}_s$. For notational convenience, we have neglected the symbol “ δ ” in the

expression of quantum fluctuation operators in Eqs. (13) and (14). We also note that in the weak COM coupling regime, the steady-state mean value of the optical mode is much larger than those of the mechanical modes, i.e., $|\bar{c}_s| \gg |\bar{b}_j|$. Therefore, under this condition, the terms \hat{c}_s^2 and $\hat{c}_s^{\dagger 2}$, whose coefficient β_p is proportional to \bar{b}_j , can be safely ignored in Hamiltonian (13). Then, the Hamiltonian (13) can be reduced to

$$\begin{aligned} \tilde{H}_{lin} \simeq & \Delta_s \hat{c}_s^\dagger \hat{c}_s + \omega_{m,1} \hat{b}_1^\dagger \hat{b}_1 + \omega_{m,2} \hat{b}_2^\dagger \hat{b}_2 + (\nu \hat{b}_1^\dagger \hat{b}_2 + \nu^* \hat{b}_2^\dagger \hat{b}_1) \\ & - (\Lambda_1 \hat{c}_s^\dagger + \Lambda_1^* \hat{c}_s) (\hat{b}_1^\dagger + \hat{b}_1) - (\Lambda_2 \hat{c}_s^\dagger + \Lambda_2^* \hat{c}_s) (\hat{b}_2^\dagger + \hat{b}_2), \end{aligned} \quad (16)$$

where $\nu = \chi e^{-i\varphi}$. In our following numerical calculations, for ensuring the validity of Eq. (16), the parameters have been strictly restricted to satisfy the condition of weak COM coupling.

Moreover, as shown in Ref. [60], the ability of squeezed COM system to regulate its intracavity field intensity by adjusting the squeezing parameters provides a feasible and efficient way to enhance the strength of light-mirror interaction. To clearly see this, an enhancement factor η_j , quantifying the amount by which the effective COM coupling strength is enhanced in comparison with that of the conventional COM system, is defined as

$$\eta_j = |\Lambda_j / G_j|. \quad (17)$$

Under the condition of equal single-photon COM coupling strength, i.e., $g_1/g_2 = 1$, we have $\eta_1 = \eta_2 = \eta$. In Fig. 1(c), η is plotted as a function of the squeezing strength r_d and the squeezing reference angle θ_d . Here, G_j has been assumed to be real, which can be achieved by choosing a suitable phase of \bar{c}_s through tuning the phase reference of the cavity field. Interestingly, it is seen that by properly adjusting the squeezing parameters of the squeezed intracavity mode, e.g., when choosing $r_d = 1$ and $\theta_d = \pi$ or 3π , the maximum value of η can reach up to ~ 7 , indicating that the effective COM coupling strength Λ_j are improved by 7 times in comparison with that of the conventional COM system.

III. ENHANCING BIPARTITE AND TRIPARTITE ENTANGLEMENT UNDER THE PHASE-MATCHED CONDITION

As discussed above, we derive an effective theoretical model for the squeezed COM system. In this section, based on this model, we study how to generate, manipulate, and even enhance the bipartite light-mirror and mirror-mirror entanglement, as well as the full tripartite entanglement. For this purpose, we shall first calculate the covariance matrix (CM) for the squeezed COM system, by which one can quantify the bipartite and tripartite entanglement through introducing proper entanglement measures, e.g., the logarithmic negativity and the minimum residual contangle. Then, based on numerical calculations of such measures, we will qualitatively and quantitatively discuss some specific cases with regard to the coherent generation and manipulation of entanglement in squeezed COM systems, and show its advantages on the achievement

of enhanced bipartite and tripartite entanglement under the phase-matched condition.

A. Covariance matrix and quantitative entanglement measures for squeezed COM systems

In our proposed scheme, due to the linearized dynamics and the Gaussian nature of the optical and mechanical input noises, the steady state of the squeezed COM system, independently of any initial condition, could eventually evolve into a tripartite zero-mean Gaussian state, whose statistic is commonly characterized by a Wigner function with multivariate normal distribution on phase space, i.e.,

$$W(\psi) = \frac{\exp\left[-\frac{1}{2}(\psi^\dagger V^{-1} \psi)\right]}{\pi^2 \sqrt{\det(V)}}. \quad (18)$$

Here $\psi = (\hat{X}, \hat{Y}, \hat{Q}_1, \hat{P}_1, \hat{Q}_2, \hat{P}_2)^T$ is the vector of optical and mechanical quadrature operators, with its components defined by

$$\begin{aligned} X &= \frac{1}{\sqrt{2}} (\hat{c}_s^\dagger + \hat{c}_s), & Y &= \frac{i}{\sqrt{2}} (\hat{c}_s^\dagger - \hat{c}_s), \\ Q_j &= \frac{1}{\sqrt{2}} (\hat{b}_j^\dagger + \hat{b}_j), & P_j &= \frac{i}{\sqrt{2}} (\hat{b}_j^\dagger - \hat{b}_j). \end{aligned} \quad (19)$$

Also, V denotes the steady-state CM of the squeezed COM system, and its matrix element is given by

$$V_{kl} = \langle \psi_k \psi_l + \psi_l \psi_k \rangle / 2, \quad (k, l = 1, 2, \dots, 6). \quad (20)$$

By grouping together the quantum correlation functions for bosonic operators in a vector, $X = (x_1, x_2, \dots, x_{24})^T$, one can obtain its time evolution equation from Eq. (14), i.e.,

$$\frac{d}{dt} X = M \cdot X + N, \quad (21)$$

where

$$\begin{aligned} N &= [\kappa N_s, \kappa(N_s + 1), \gamma_{m,1} \bar{n}_{m,1}, \gamma_{m,1}(\bar{n}_{m,1} + 1), \\ & \quad \gamma_{m,2} \bar{n}_{m,2}, \gamma_{m,2}(\bar{n}_{m,2} + 1), \kappa M_s^*, \kappa M_s, 0, 0, \\ & \quad 0, 0, 0, 0, 0, 0, 0, 0, 0, 0, 0, 0]^T, \end{aligned} \quad (22)$$

is a vector involving the correlation functions for the input quantum noises. Here the exact expression for the coefficient matrix M and the detailed derivation process of the time evolution equation (21) are too cumbersome, and, for convenience, we have reported them in the Supporting Information. Notably, by numerically solving Eq. (21) and using the relations between bosonic operators and quadrature operators, one can directly obtain the steady-state CM V .

Regarding the verification of the fundamental entanglement property in our proposed scheme, we adopt here the logarithmic negativity $E_{\mathcal{N}}$ and the minimum residual contangle $\mathcal{R}_{\tau}^{\min}$ as quantitative measures for certifying the bipartite and tripartite entanglement, respectively, which are defined based on

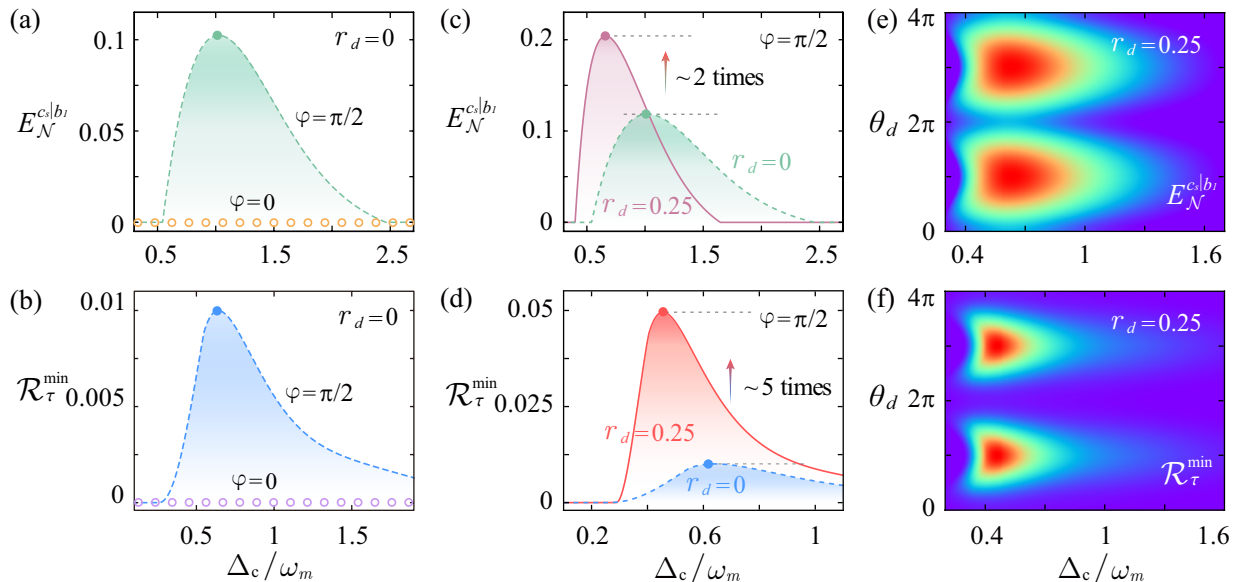


FIG. 2. Enhancement of bipartite light-mirror entanglement and full tripartite entanglement under the phase-matched condition achieving at $\delta r = 0$ and $\delta\theta = \pm n\pi$ ($n = 1, 3, 5, \dots$). (a, c) The logarithmic negativity $E_{\mathcal{N}}^{c_s|b_l}$ and (b, d) the minimum residual contangle $\mathcal{R}_{\tau}^{\min}$ versus the scaled optical detuning Δ_c/ω_m for different values of squeezing strength r_d , with squeezing reference angle $\theta_d = \pi$. For $r_d = 0$, $E_{\mathcal{N}}^{c_s|b_l}$ and $\mathcal{R}_{\tau}^{\min}$ can achieve their maximum values when breaking the dark mode effect at $\varphi = \pi/2$. For $r_d = 0.25$, with respect to the case of DMB at $\varphi = \pi/2$, the maximum values of $E_{\mathcal{N}}^{c_s|b_l}$ and $\mathcal{R}_{\tau}^{\min}$ are further enhanced by about 2 and 5 times, respectively. (e, f) Density plot of $E_{\mathcal{N}}^{c_s|b_l}$ and $\mathcal{R}_{\tau}^{\min}$ as a function of the scaled optical detuning Δ_c/ω_m and the squeezing reference angle θ_d , with squeezing strength $r_d = 0.25$. Other parameters are chosen as those in Fig. 1.

specifying the positivity of the partial transpose of the states. Considering that both optical and mechanical modes of this squeezed COM system are continuous variables (CV), the logarithmic negativity $E_{\mathcal{N}}$ is defined as [82]

$$E_{\mathcal{N}} = \max [0, -\ln(2\eta_0^-)], \quad (23)$$

where $\eta_0^- \equiv 2^{-1/2} \{[\Sigma(V_{\mu\nu}) - [\Sigma(V_{\mu\nu})^2 - 4 \det V_{\mu\nu}]^{1/2}]^{1/2}\}$, with $\Sigma(V_{\mu\nu}) \equiv \det \mathcal{A}_{\mu} + \det \mathcal{B}_{\nu} - 2 \det \mathcal{C}_{\mu\nu}$, is the minimum symplectic eigenvalue of the partial transpose of a reduced 4×4 CM $V_{\mu\nu}$. The indexes μ and ν label the two selected modes under consideration, and the reduced CM $V_{\mu\nu}$ contains the entries of V associated with the corresponding bipartitions μ and ν . By removing the rows and columns of the unwanted modes in V , the reduced CM $V_{\mu\nu}$ can be straightforwardly obtained, which has a 2×2 block form given by

$$V_{\mu\nu} = \begin{pmatrix} \mathcal{A}_{\mu} & \mathcal{C}_{\mu\nu} \\ \mathcal{C}_{\mu\nu}^T & \mathcal{B}_{\nu} \end{pmatrix}. \quad (24)$$

Equation (23) indicates that the selected bipartition μ and ν gets entangled if and only if $\eta_0^- < 1/2$, which is equivalent to Simon's necessary and sufficient entanglement nonpositive partial transpose criterion (or the related Peres-Horodecki criterion) for certifying bipartite entanglement in Gaussian states [83].

Furthermore, the minimum residual contangle, $\mathcal{R}_{\tau}^{\min}$, which provides a *bona fide* quantification of CV tripartite entanglement, is commonly defined as

$$\mathcal{R}_{\tau}^{\min} = \min_{(r,s,t)} [E_{\tau}^{r|st} - E_{\tau}^{r|s} - E_{\tau}^{r|t}], \quad (25)$$

where $(r, s, t) \in \{c_s, b_1, b_2\}$ denotes all the possible permutations of the three-mode indexes. $E_{\tau}^{u|v}$ is the contangle of subsystems of u (u contains one mode) and v (v contains one or two modes), which can be defined by a proper entanglement monotone, e.g., the squared logarithmic negativity. Based on Eq. (23), the one-mode-vs-one-mode contangle $E_{\tau}^{r|s}$ and $E_{\tau}^{r|t}$ can be directly obtained by employing its definition, namely, $E_{\tau} \equiv [E_{\mathcal{N}}]^2$. However, when calculating the one-mode-vs-two-modes contangle $E_{\tau}^{r|st}$, one must alter the basic definition of Eq. (23) by rewriting the definition of η_0^- as given by $\eta_0^- \equiv \min [\text{eig}[i\Omega_3 \tilde{V}_{r|st}]]$, where η_0^- becomes the minimum symplectic eigenvalue of the partial transpose of a 6×6 CM V , with $\Omega_3 = \oplus_{k=1}^3 i\sigma_y$ and σ_y the y -Pauli matrix. $\tilde{V}_{r|st}$ corresponds to the partial transpose of V , which connects to V with the relation of $\tilde{V}_{r|st} = P_{r|st} V P_{r|st}$, and $P_{r|st} = \text{diag}(1, -1, 1, 1, 1, 1)$ is the partial transposition matrix. In terms of $E_{\tau}^{s|rt}$ and $E_{\tau}^{t|sr}$, the corresponding partial transpose matrices are given by $P_{s|rt} = \text{diag}(1, 1, 1, -1, 1, 1)$ and $P_{t|sr} = \text{diag}(1, 1, 1, 1, 1, -1)$, respectively. In addition, according to the Coffman-Kundu-Wootters monogamy inequality for quantum entanglement, we also note that the residual contangle is required to satisfy the following monogamy condition, i.e., $E_{\tau}^{r|st} - E_{\tau}^{r|s} - E_{\tau}^{r|t} \geq 0$, which means that the bipartite entanglement between the partition r and the remaining two partitions st is never smaller than the sum of the $r|s$ and $r|t$ bipartite entanglements in the reduced states. As such, if there are nonzero values of the minimum residual contangle, i.e., $\mathcal{R}_{\tau}^{\min} > 0$, one can verify that the full tripartite entangle-

ment is present for the CV system.

B. Numerical verification of the bipartite and tripartite entanglement in squeezed COM systems

In the previous sections, as demonstrated in Figs. 1(b) and 1(c), we have shown that the squeezed COM system can provide an efficient method to regulate both the light-mirror interaction and the light-reservoir interaction, which thus allows us to enhance the effective COM coupling strength while suppress the effective optical input noises by choosing proper squeezing parameters. Hereafter, we start to explore how to coherently generate and manipulate entanglement by harnessing this unique property of the squeezed COM system. For evaluating entanglement measures, we can numerically calculate the steady-state CM V by solving Eq. (21) through using the following scaled parameters: $\omega_{m,j}/\omega_m = 1$, $\kappa/\omega_m = 0.9$, $\gamma_{m,j}/\omega_m = 10^{-5}$, $g_j/\omega_m = 0.2$, $\chi/\omega_m = 0.1$, $\bar{n}_{m,j} = 100$. Here we assume the same parameters for two identical mechanical mirrors, which ensures that the two types of light-mirror entanglement ($E_{\mathcal{N}}^{c_s|b_1}$ and $E_{\mathcal{N}}^{c_s|b_2}$) in our proposed scheme have similar behaviors with the variation of the controlling parameters. Based on this assumption, for convenience, we only study the behavior of $E_{\mathcal{N}}^{c_s|b_1}$ as an example in the following discussion. Also, we note that the values of the squeezing parameters r_d and r_e have been chosen ranging from about 0.01 to 1 in such calculations, which corresponds to a ratio for Ξ_d/Δ_c estimated on the order of $10^{-3} \sim 10^{-1}$. We stress that, for FP cavities, ω_m is typically $10^{-3} - 10^3$ MHz, and thus to satisfy the above condition for Ξ_d/Δ_c around the COM resonance region (i.e., $\Delta_c/\omega_m \simeq 1$), it requires the order of Ξ_d ranging from 10^{-6} to 10^2 MHz, which is feasible for current experimental techniques [84, 85].

In Figs. 1 and 2, we first show how to regulate the behavior of bipartite and tripartite entanglement involving one mechanical mirror, which is achieved by adjusting the squeezing parameters of the squeezed intracavity mode and the injected squeezed laser field. Figure 1(d) shows the logarithmic negativity $E_{\mathcal{N}}^{c_s|b_1}$ as a function of the reference angle θ_d of the squeezed intracavity mode, with $\delta r = 0$ and $\delta\theta = \pi$. One can intuitively see that in the absence of intracavity squeezing (i.e., $r_d = 0$), $E_{\mathcal{N}}^{c_s|b_1}$ remains unchange with the variation of θ_d , whose value always corresponds to a constant of about 0.041. In contrast, when introducing the squeezed intracavity mode via OPA (i.e., $r_d = 0.25$), $E_{\mathcal{N}}^{c_s|b_1}$ starts to oscillate back and forth periodically over θ_d with an approximate periodicity of 2π . Moreover, the maximum value of $E_{\mathcal{N}}^{c_s|b_1}$ can reach up to about 0.185 in this case, which is enhanced by 4.5 times compared to that of the conventional COM system. This result indicates that our proposed scheme is poised to provide a promising platform for achieving the enhanced and controllable entangled states by coherently adjusting the reference angle of the squeezed intracavity mode, which we will discuss in detail later. The underlying physics of this phenomenon is due to the fact that the light-mirror entanglement is a monotonically increasing function of the effective

COM coupling strength Λ_j , which, as shown in Fig. 1(c), are effectively regulated by the squeezing parameters of the intracavity field. Then, for the squeezing parameters that can enhance the light-mirror interaction strength, it can correspondingly improve the light-mirror entanglement. However, it should be stressed that this procedure for entanglement manipulation and enhancement requires to be performed under the phase-matched condition, i.e., satisfying $\delta r = 0$ and $\delta\theta = \pm n\pi$ ($n = 1, 3, 5, \dots$). To clearly see this, as demonstrated in Fig. 1(e), we plot the logarithmic negativity $E_{\mathcal{N}}^{c_s|b_1}$ as a function of the phase difference $\delta\theta$, with $r_d = 0.25$ and $\theta_d = 0$. It is obviously seen that $E_{\mathcal{N}}^{c_s|b_1}$ are highly peaked within a finite interval of values of $\delta\theta$ around $\delta\theta \simeq \pi$ or 3π , showing that the light-mirror entanglement is sensitive to the variation of $\delta\theta$ and survives only around the phase-matched condition. Physically, this result can be understood as follows. The effective optical input noises N_s and M_s can only be suppressed completely when the phase-matched condition is fulfilled, whereas they would exponentially increase with other squeezing parameters, something we discussed in detail in Sec. II. On the other hand, when the optical input noises increase, the light-mirror entanglement commonly tends to be inhibited or even vanish. Therefore, it becomes a necessary condition for our proposed scheme to fulfill the phase-matched condition.

By assuming the fulfillment of the phase-matched condition, we further explore in detail how to achieve an enhancement of both bipartite light-mirror entanglement and full tripartite entanglement with respect to some specific squeezing parameters. In Figs. 2(a)-2(d), we plot the logarithmic negativity $E_{\mathcal{N}}^{c_s|b_1}$ and the minimum residual contangle \mathcal{R}_τ^{\min} as a function of the optical detuning Δ_c for different values of r_d , with $\theta_d = \pi$, $\delta r = 0$, and $\delta\theta = \pi$. From Figs. 2(a) and 2(b), it is clearly seen that for the familiar case without any intracavity squeezing (i.e., $r_d = 0$), to entangle an optical radiation field with mechanical mirrors in a three-mode COM system with bilinear cyclic couplings, one should first break the dark mode effect through choosing a proper phase φ of the phonon-hopping interactions, which has already been revealed in some preceding studies [21, 45, 50, 51, 86]. Note that here, in the case of $\varphi = k\pi$ ($k = 0, 1, 2, \dots$), both bipartite light-mirror entanglement and full tripartite entanglement are absent, that is, $E_{\mathcal{N}}^{c_s|b_1} = 0$ and $\mathcal{R}_\tau^{\min} = 0$, which corresponds to a situation of the dark-mode-unbroken (DMU) regime. In contrast, when choosing other values of φ , such bipartite and tripartite entanglement can simultaneously emerge and reach their maximum values at an optimal phase angle of $\varphi = \pi/2$, which corresponds to a situation of the dark-mode-broken (DMB) regime. From these results, it is found that the entanglement, especially the tripartite one, are severely restricted even in the DMB regime, which results from the limitation of weak light-mirror coupling strength of the conventional COM system. Interestingly, as shown in Figs. 2(c) and 2(d), one can find that by harnessing the unique features of the squeezed COM systems (with, e.g., squeezing strength $r_d = 0.25$), a considerable enhancement of both bipartite light-mirror entanglement and full tripartite entanglement can be achieved by about 2 or

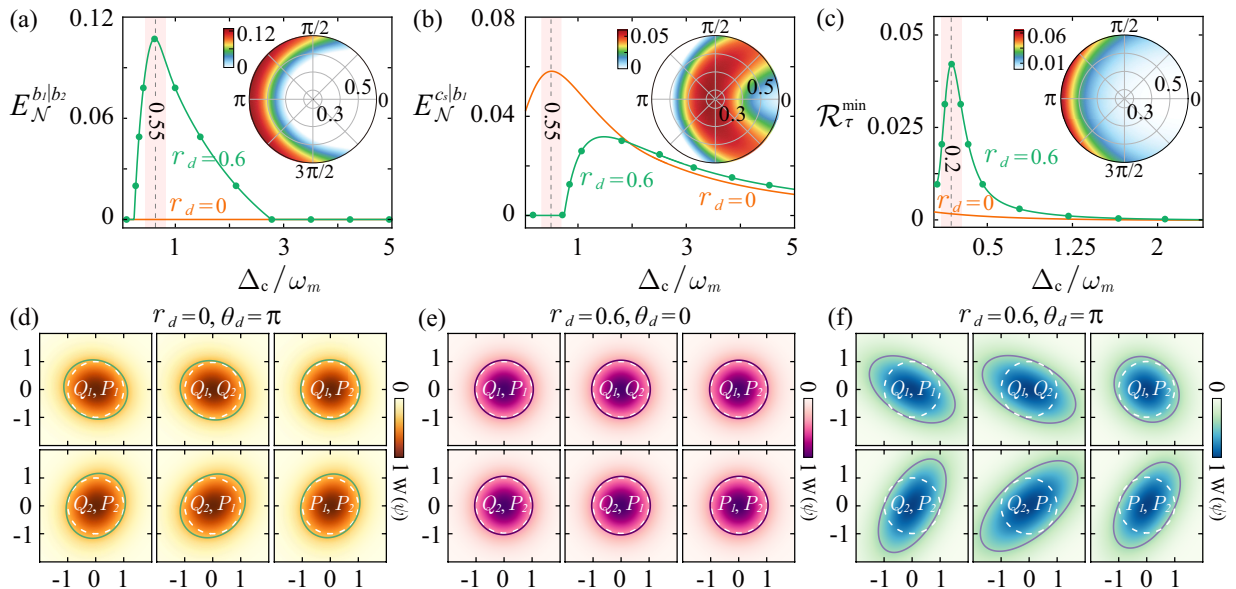


FIG. 3. Entanglement and the associated quadrature squeezing with respect to the subsystem of two mechanical mirrors. The logarithmic negativity (a) $E_{\mathcal{N}}^{b_1|b_2}$, (b) $E_{\mathcal{N}}^{c_s|b_1}$, and (c) the minimum residual contangle $\mathcal{R}_{\tau}^{\min}$ versus the scaled optical detuning Δ_c/ω_m for different values of squeezing strength r_d , with squeezing reference angle $\theta_d = \pi$. The inserts show the dependence of $E_{\mathcal{N}}^{b_1|b_2}$, $E_{\mathcal{N}}^{c_s|b_1}$, and $\mathcal{R}_{\tau}^{\min}$ on the squeezing strength r_d and the squeezing reference angle θ_d at the optical detuning $\Delta_c/\omega_m = 0.55, 0.55, 0.2$, respectively. (d)-(f) Reconstructed Wigner function $W(\psi)$ for the steady state of two mechanical modes at the optical detuning $\Delta_c/\omega_m = 0.55$, with respect to the case for different values of squeezing strength r_d and squeezing reference angle θ_d , along with that of an ideal vacuum state for reference. Each panel corresponds to a characteristic projection of $W(\psi)$ on two-dimensional subspaces within $\psi = (\hat{X}, \hat{Y}, \hat{Q}_1, \hat{P}_1, \hat{Q}_2, \hat{P}_2)^T$, which is obtained by integrating out the other four quadratures in ψ . The solid (dashed) line indicates a drop by $1/e$ of the maximum value of $W(\psi)$ for the relevant steady (vacuum) state. The legends ψ_i, ψ_j in each panel are corresponding to a correlation with ψ_i along the x axis and ψ_j along the y axis. The parameters are chosen as follows: $\gamma_{m,j}/\omega_m = 0.2, g_j/\omega_m = 0.1, \bar{n}_{m,j} = 0.05$. Other parameters are chosen as those in Fig. 1.

5 times, respectively. Moreover, as shown in Figs. 2(e) and 2(f), the degree of such bipartite and tripartite entanglement also relies on the squeezing reference angle θ_d and can reach their maximum values at the optimal angle $\theta_d = \pi$ or 3π , which is consistent with the previous discussions in Fig. 1. This result implies that for the sake of enhancing entanglement in squeezed COM systems, one should properly choose parameters both for squeezing strength r_d and for squeezing reference angle θ_d .

Finally, we present how to regulate the behaviors of bipartite and tripartite entanglement involving two mechanical mirrors. For this purpose, we plot the corresponding entanglement measures and the associated reconstructed Wigner function in Fig. 3, where we have altered the following parameters as: $\gamma_{m,j}/\omega_m = 0.2, g_j/\omega_m = 0.1, \bar{n}_{m,j} = 0.05$. Specifically, as shown in Figs. 3(a)-3(c), the logarithmic negativity $E_{\mathcal{N}}^{b_1|b_2}$, $E_{\mathcal{N}}^{c_s|b_1}$, and the minimum residual contangle $\mathcal{R}_{\tau}^{\min}$ are plotted as a function of the optical detuning Δ_c for different values of r_d , with $\theta_d = \pi, \delta r = 0$, and $\delta\theta = \pi$. It is seen that in the case of a conventional COM system without any intracavity squeezing (i.e., $r_d = 0$), the bipartite mirror-mirror entanglement is not present, i.e., $E_{\mathcal{N}}^{b_1|b_2} = 0$, whereas the bipartite light-mirror entanglement exists and reaches its maximum at $\Delta_c/\omega_m = 0.55$, i.e., $E_{\mathcal{N}}^{c_s|b_1} = 0.059$. As a result, the full tripartite entanglement is too weak in this case. In contrast, it is remarkable that by using a squeezed COM

system with squeezing strength $r_d = 0.6$ and squeezing reference angle $\theta_d = \pi$, the bipartite mirror-mirror entanglement can emerge, where the associated $E_{\mathcal{N}}^{b_1|b_2}$ achieves a considerable maximum value of about $E_{\mathcal{N}}^{b_1|b_2} = 0.11$. Correspondingly, the full tripartite entanglement is significantly enhanced as well, and the profile of $\mathcal{R}_{\tau}^{\min}$ is characterized by a sharp peak with its maximum value of about $\mathcal{R}_{\tau}^{\min} = 0.044$ around the optical detuning $\Delta_c/\omega_m = 0.2$. Moreover, it is also seen that the light-mirror entanglement $E_{\mathcal{N}}^{c_s|b_1}$ is suppressed when the mirror-mirror entanglement emerges, resulting from the complementary distribution of entanglement. To clearly see this phenomenon, we further plot the dependence of the entanglement measures on squeezing parameters r_d and θ_d in the inserted figure of Figs. 3(a)-3(c). The result indicates that in the case of a small squeezing strength, the light field tends to be strongly entangled with the mirror, and there is neither mirror-mirror entanglement nor full tripartite entanglement. However, as the squeezing strength increases, the initial light-mirror entanglement can be partially or even totally transferred to the mirror-mirror subsystem, which leads to a significant enhancement of the full tripartite entanglement. Moreover, it is seen that due to the complementary distribution of the entanglement, the initial light-mirror entanglement $E_{\mathcal{N}}^{c_s|b_1}$ is suppressed as it is partially transferred to the mirror-mirror subsystem. We also show the dependence of

the entanglement measures on squeezing parameters r_d and θ_d in the inserted figure of Figs. 3(a)-3(c), which demonstrates a more clear complementary distribution of the entanglement. In Figs. 3(d)-3(f), we plot a selection of characteristic projections of the reconstructed Wigner function $W(\psi)$ on two-dimensional subspaces with $\Delta_c/\omega_m = 0.55$, $\delta r = 0$, and $\delta\theta = \pi$, showing the quadrature statistics for the two mechanical mirrors with respect to different squeezing parameters. The ellipse (circle) with solid (dashed) line corresponds to a drop by $1/e$ of the maximum value of $W(\psi)$ for the steady (vacuum) state of the system. Note that when the boundary of the ellipse enters the circle, it indicates the existence of a squeezed state, where the variance of the relevant steady state of the system is smaller than that of a vacuum state. In the absence of intracavity squeezing, i.e., $r_d = 0$, it is found that none of the characteristic projections of $W(\psi)$ is characterized by squeezing correlation for the quadrature pairs of the two mechanical mirrors [see Fig. 3(d)]. Meanwhile, in the presence of intracavity squeezing, i.e., $r_d = 0.6$, it is found that the emergence of quadrature squeezing depends on the option of squeezing reference angle θ_d . For example, when choosing $\theta_d = 0$, the projections of $W(\psi)$ for all possible permutations of quadrature pairs is consistent with a Gaussian distribution of large variance, resulting from the phase-preserving amplification of the vacuum state [see Fig. 3(e)]. Nevertheless, when choosing $\theta_d = \pi$, the projection of $W(\psi)$ for local quadrature pairs $\{Q_1, P_1\}$, $\{Q_2, P_2\}$ and for cross-quadrature pairs $\{P_1, P_2\}$ are squeezed along the diagonal direction, indicating that both single-mode and two-mode squeezing correlations emerge for the associated mechanical mirrors [see Fig. 3(f)]. These results are consistent with the features of the mirror-mirror entanglement previously shown in Figs. 3(a)-3(c).

IV. CONCLUSION

In summary, we have presented a theoretical proposal to achieve enhanced and controllable light-mirror, mirror-mirror and full tripartite entanglement in a squeezed COM system, which consists of a FP cavity with two movable mirrors, a nonlinear $\chi^{(2)}$ medium, and an injected broadband squeezed laser field. The nonlinear $\chi^{(2)}$ medium serves as an OPA that enables a squeezed intracavity mode for the COM system. Meanwhile, the injected broadband squeezed laser field can act as a squeezed vacuum reservoir. We show that the interplay of the squeezed intracavity mode and the squeezed vacuum reservoir allows us to effectively enhance the light-mirror interaction while suppress the optical input noises by

choosing proper squeezing parameters, where the fulfillment of the phase-matched condition that achieves at $\delta r = 0$ and $\delta\theta = \pm n\pi$ ($n = 1, 3, 5, \dots$) plays a key role in this procedure. More interestingly, we find that these features of squeezed COM system provide an appealing method to coherently generate, manipulate and enhance the light-mirror, mirror-mirror and full tripartite entanglement, as well as the associated single-mode or two-mode quadrature squeezing. We remark that our work reveals the potential applications of the squeezed COM system to engineer various quantum COM effects, such as photon blockade [60, 65–67, 75], quantum squeezing [64, 74, 86], quantum phase transition [72], and optical or mechanical cat state [62, 63, 87], to name a few. Also, our work holds the promise to provide a controllable quantum resource for a wide range of entanglement-based quantum technologies, including quantum computing [2], quantum sensing [6–8] and quantum networking [3–5]. Moreover, although we have considered here a specific case of a squeezed COM system, we envision that our proposal can be extended to a lot of other optical platforms to regulate their light-matter interaction, such as those involving atoms [14–16], magnons [43, 68], and superconducting circuits [17, 18].

V. ACKNOWLEDGMENT

The authors thank Wei Qin, Deng-Gao Lai, and Jian Huang for helpful discussions. H.J. is supported by the National Natural Science Foundation of China (NSFC, Grant No. 11935006), the National Key R&D Program of China (Grant No. 2024YFE0102400), the Hunan Provincial Major Sci-Tech Program (Grant No. 2023ZJ1010) and the Science and Technology Innovation Program of Hunan Province (Grant No. 2020RC4047). L.-M.K. is supported by the NSFC (Grants No. 12247105, 11935006 and 12175060), Hunan Provincial Major Sci-Tech Program (Grant No. 2023ZJ1010), and Henan Science and Technology Major Project (No. 241100210400). J.-Q.L. was supported in part by the NSFC (Grants No. 12175061, No. 12247105, and No. 11935006), the National Key R&D Program of China (Grant No. 2024YFE0102400), and the Hunan Provincial Major Sci-Tech Program (Grant No. 2023ZJ1010). Y.-F.J. is supported by the NSFC (Grant No. 12147156). Y.W. is supported by the NSFC (Grant No. 12205256) and the Henan Provincial Science and Technology Research Project (Grant No. 232102221001). W.L. is supported by the NSFC (Grant No. 12205092) and the Hunan Provincial Natural Science Foundation of China (Grant No. 2023JJ40208).

-
- [1] R. Horodecki, P. Horodecki, M. Horodecki, and K. Horodecki, Quantum entanglement, *Rev. Mod. Phys.* **81**, 865 (2009).
[2] X. Zhang, H.-O. Li, G. Cao, M. Xiao, G.-C. Guo, and G.-P. Guo, Semiconductor quantum computation, *Natl. Sci. Rev.* **6**, 32 (2018).
[3] F. Xu, X. Ma, Q. Zhang, H.-K. Lo, and J.-W. Pan, Secure quantum key distribution with realistic devices, *Rev. Mod. Phys.* **92**,

- 025002 (2020).
[4] H. J. Kimble, The quantum internet, *Nature (London)* **453**, 1023 (2008).
[5] M. C. Kuzyk and H. Wang, Scaling Phononic Quantum Networks of Solid-State Spins with Closed Mechanical Subsystems, *Phys. Rev. X* **8**, 041027 (2018).

- [6] C. L. Degen, F. Reinhard, and P. Cappellaro, Quantum sensing, *Rev. Mod. Phys.* **89**, 035002 (2017).
- [7] R. Fleury, D. Sounas, and A. Alù, An invisible acoustic sensor based on parity-time symmetry, *Nat. Commun.* **6**, 5905 (2015).
- [8] W. Zhao, S.-D. Zhang, A. Miranowicz, and H. Jing, Weak-force sensing with squeezed optomechanics, *Sci. China Phys. Mech. Astron.* **63**, 224211 (2020).
- [9] N. Friis, G. Vitagliano, M. Malik, and M. Huber, Entanglement certification from theory to experiment, *Nat. Rev. Phys.* **1**, 72 (2019).
- [10] X.-C. Yao, T.-X. Wang, P. Xu, H. Lu, G.-S. Pan, X.-H. Bao, C.-Z. Peng, C.-Y. Lu, Y.-A. Chen, and J.-W. Pan, Observation of eight-photon entanglement, *Nat. Photonics* **6**, 225 (2012).
- [11] X.-L. Wang, L.-K. Chen, W. Li, H.-L. Huang, C. Liu, C. Chen, Y.-H. Luo, Z.-E. Su, D. Wu, Z.-D. Li, H. Lu, Y. Hu, X. Jiang, C.-Z. Peng, L. Li, N.-L. Liu, Y.-A. Chen, C.-Y. Lu, and J.-W. Pan, Experimental Ten-Photon Entanglement, *Phys. Rev. Lett.* **117**, 210502 (2016).
- [12] H. Häffner, W. Hänsel, C. F. Roos, J. Benhelm, D. Chek-al-kar, M. Chwalla, T. Körber, U. D. Rapol, M. Riebe, P. O. Schmidt, C. Becher, O. Gühne, W. Dür, R. Blatt, Scalable multiparticle entanglement of trapped ions, *Nature (London)* **438**, 643 (2005).
- [13] A. Stute, B. Casabone, P. Schindler, T. Monz, P. O. Schmidt, B. Brandstetter, T. E. Northup, and R. Blatt, Tunable ion-photon entanglement in an optical cavity, *Nature (London)* **485**, 482 (2012).
- [14] H.-N. Dai, B. Yang, A. Reingruber, X.-F. Xu, X. Jiang, Y.-A. Chen, Z.-S. Yuan, and J.-W. Pan, Generation and detection of atomic spin entanglement in optical lattices, *Nat. Phys.* **12**, 783 (2016).
- [15] T. M. Karg, B. Gouraud, C. T. Ngai, G.-L. Schmid, K. Hammerer, and P. Treutlein, Light-mediated strong coupling between a mechanical oscillator and atomic spins 1 meter apart, *Science* **369**, 174 (2020).
- [16] X.-Y. Luo, Y. Yu, J.-L. Liu, M.-Y. Zheng, C.-Y. Wang, B. Wang, J. Li, X. Jiang, X.-P. Xie, Q. Zhang, X.-H. Bao, and J.-W. Pan, Postselected Entanglement between Two Atomic Ensembles Separated by 12.5 km, *Phys. Rev. Lett.* **129**, 050503 (2022).
- [17] P. Campagne-Ibarcq, E. Zaly-Geller, A. Narla, S. Shankar, P. Reinhold, L. Burkhardt, C. Axline, W. Pfaff, L. Frunzio, R. J. Schoelkopf, and M. H. Devoret, Deterministic Remote Entanglement of Superconducting Circuits through Microwave Two-Photon Transitions, *Phys. Rev. Lett.* **120**, 200501 (2018).
- [18] P. Kurpiers, P. Magnard, T. Walter, B. Royer, M. Pechal, J. Heinsoo, Y. Salathé, A. Akin, S. Storz, J.-C. Besse, S. Gasparinetti, A. Blais, and A. Wallraff, Deterministic quantum state transfer and remote entanglement using microwave photons, *Nature (London)* **558**, 264 (2018).
- [19] A. D. O’Connell, M. Hofheinz, M. Ansmann, R. C. Bialczak, M. Lenander, E. Lucero, M. Neeley, D. Sank, H. Wang, M. Weides, J. Wenner, J. M. Martinis, and A. N. Cleland, Quantum ground state and single-phonon control of a mechanical resonator, *Nature (London)* **464**, 697 (2010).
- [20] D.-G. Lai, F. Zou, B.-P. Hou, Y.-F. Xiao, and J.-Q. Liao, Simultaneous cooling of coupled mechanical resonators in cavity optomechanics, *Phys. Rev. A* **98**, 023860 (2018).
- [21] J. Huang, D.-G. Lai, C. Liu, J.-F. Huang, F. Nori, and J.-Q. Liao, Multimode optomechanical cooling via general dark-mode control, *Phys. Rev. A* **106**, 013526 (2022).
- [22] M. Aspelmeyer, T. J. Kippenberg, and F. Marquardt, Cavity optomechanics, *Rev. Mod. Phys.* **86**, 1391 (2014).
- [23] H. Xiong, L.-G. Si, X.-Y. Lü, X.-X. Yang, and Y. Wu, Review of cavity optomechanics in the weak-coupling regime: from linearization to intrinsic nonlinear interactions, *Sci. China Phys. Mech. Astron.* **58**, 1 (2015).
- [24] S. Barzanjeh, A. Xuereb, S. Gröblacher, M. Paternostro, C. A. Regal, and E. M. Weig, Optomechanics for quantum technologies, *Nat. Phys.* **18**, 15 (2022).
- [25] D. Vitali, S. Gigan, A. Ferreira, H. R. Böhm, P. Tombesi, A. Guerreiro, V. Vedral, A. Zeilinger, and M. Aspelmeyer, Optomechanical Entanglement between a Movable Mirror and a Cavity Field, *Phys. Rev. Lett.* **98**, 030405 (2007).
- [26] T. A. Palomaki, J. D. Teufel, R. W. Simmonds, and K. W. Lehnert, Entangling Mechanical Motion with Microwave Fields, *Science* **342**, 710 (2013).
- [27] R. Ghobadi, S. Kumar, B. Pepper, D. Bouwmeester, A. I. Lvovsky, and C. Simon, Optomechanical Micro-Macro Entanglement, *Phys. Rev. Lett.* **112**, 080503 (2014).
- [28] R. Riedinger, S. Hong, R. A. Norte, J. A. Slater, J. Shang, A. G. Krause, V. Anant, M. Aspelmeyer, and S. Gröblacher, Non-classical correlations between single photons and phonons from a mechanical oscillator, *Nature (London)* **530**, 313 (2016).
- [29] I. Marinković, A. Wallucks, R. Riedinger, S. Hong, M. Aspelmeyer, and S. Gröblacher, Optomechanical Bell Test, *Phys. Rev. Lett.* **121**, 220404 (2018).
- [30] H. Tan and G. Li, Multicolor quadripartite entanglement from an optomechanical cavity, *Phys. Rev. A* **84**, 024301 (2011).
- [31] S. Barzanjeh, E. S. Redchenko, M. Peruzzo, M. Wulf, D. P. Lewis, G. Arnold, and J. M. Fink, Stationary entangled radiation from micromechanical motion, *Nature (London)* **570**, 480 (2019).
- [32] J. Chen, M. Rossi, D. Mason, and A. Schliesser, Entanglement of propagating optical modes via a mechanical interface, *Nat. Commun.* **11**, 943 (2020).
- [33] M. J. Hartmann and M. B. Plenio, Steady State Entanglement in the Mechanical Vibrations of Two Dielectric Membranes, *Phys. Rev. Lett.* **101**, 200503 (2008).
- [34] J.-Q. Liao, Q.-Q. Wu, and F. Nori, Entangling two macroscopic mechanical mirrors in a two-cavity optomechanical system, *Phys. Rev. A* **89**, 014302 (2014).
- [35] J. Li, I. M. Haghghi, N. Malossi, S. Zippilli, and D. Vitali, Generation and detection of large and robust entanglement between two different mechanical resonators in cavity optomechanics, *New J. Phys.* **17**, 103037 (2015).
- [36] C. F. Ockeloen-Korppi, E. Damskäg, J.-M. Pirkkalainen, M. Asjad, A. A. Clerk, F. Massel, M. J. Woolley, and M. A. Sillanpää, Stabilized entanglement of massive mechanical oscillators, *Nature (London)* **556**, 478 (2018).
- [37] R. Riedinger, A. Wallucks, I. Marinković, C. Löschnauer, M. Aspelmeyer, S. Hong, and S. Gröblacher, Remote quantum entanglement between two micromechanical oscillators, *Nature (London)* **556**, 473 (2018).
- [38] S. Kotler, G. A. Peterson, E. Shojaei, F. Lecocq, K. Cicak, A. Kwiatkowski, S. Geller, S. Glancy, E. Knill, R. W. Simmonds, J. Aumentado, and J. D. Teufel, Direct observation of deterministic macroscopic entanglement, *Science* **372**, 622 (2021).
- [39] L. Mercier de Lépinay, C. F. Ockeloen-Korppi, M. J. Woolley, and M. A. Sillanpää, Quantum mechanics-free subsystem with mechanical oscillators, *Science* **372**, 625 (2021).
- [40] S. Armstrong, J.-F. Morizur, J. Janousek, B. Hage, N. Treps, P. K. Lam, and H.-A. Bachor, Programmable multimode quantum networks, *Nat. Commun.* **3**, 1026 (2012).
- [41] Y. Cai, J. Roslund, G. Ferrini, F. Arzani, X. Xu, C. Fabre, and N. Treps, Multimode entanglement in reconfigurable graph states using optical frequency combs, *Nat. Commun.* **8**, 15645 (2017).

- [42] J. Jing, J. Zhang, Y. Yan, F. Zhao, C. Xie, and K. Peng, Experimental Demonstration of Tripartite Entanglement and Controlled Dense Coding for Continuous Variables, *Phys. Rev. Lett.* **90**, 167903 (2003).
- [43] J. Li, S.-Y. Zhu, and G. S. Agarwal, Magnon-Photon-Phonon Entanglement in Cavity Magnomechanics, *Phys. Rev. Lett.* **121**, 203601 (2018).
- [44] C. Genes, D. Vitali, and P. Tombesi, Emergence of atom-light-mirror entanglement inside an optical cavity, *Phys. Rev. A* **77**, 050307 (2008).
- [45] D.-G. Lai, J.-Q. Liao, A. Miranowicz, and F. Nori, Noise-Tolerant Optomechanical Entanglement via Synthetic Magnetism, *Phys. Rev. Lett.* **129**, 063602 (2022).
- [46] J.-X. Liu, Y.-F. Jiao, Y. Li, X.-W. Xu, Q.-Y. He, and H. Jing, Phase-controlled asymmetric optomechanical entanglement against optical backscattering, *Sci. China Phys. Mech. Astron.* **66**, 230312 (2023).
- [47] Y.-D. Wang and A. A. Clerk, Reservoir-Engineered Entanglement in Optomechanical Systems, *Phys. Rev. Lett.* **110**, 253601 (2013).
- [48] C.-J. Yang, J.-H. An, W. Yang, and Y. Li, Generation of stable entanglement between two cavity mirrors by squeezed-reservoir engineering, *Phys. Rev. A* **92**, 062311 (2015).
- [49] K. Araya-Sossa and M. Orszag, Generation of entanglement via squeezing on a tripartite-optomechanical system, *Phys. Rev. A* **108**, 012432 (2023).
- [50] D.-G. Lai, Y.-H. Chen, W. Qin, A. Miranowicz, and F. Nori, Tripartite optomechanical entanglement via optical-dark-mode control, *Phys. Rev. Res.* **4**, 033112 (2022).
- [51] J. Huang, D.-G. Lai, and J.-Q. Liao, Thermal-noise-resistant optomechanical entanglement via general dark-mode control, *Phys. Rev. A* **106**, 063506 (2022).
- [52] J. Li, G. Li, S. Zippilli, D. Vitali, and T. Zhang, Enhanced entanglement of two different mechanical resonators via coherent feedback, *Phys. Rev. A* **95**, 043819 (2017).
- [53] M. Ho, E. Oudot, J.-D. Bancal, and N. Sangouard, Witnessing Optomechanical Entanglement with Photon Counting, *Phys. Rev. Lett.* **121**, 023602 (2018).
- [54] M. Wang, X.-Y. Lü, Y.-D. Wang, J. Q. You, and Y. Wu, Macroscopic quantum entanglement in modulated optomechanics, *Phys. Rev. A* **94**, 053807 (2016).
- [55] C.-S. Hu, L.-T. Shen, Z.-B. Yang, H. Wu, Y. Li, and S.-B. Zheng, Manifestation of classical nonlinear dynamics in optomechanical entanglement with a parametric amplifier, *Phys. Rev. A* **100**, 043824 (2019).
- [56] S. Huang and A. Chen, Quadrature-squeezed light and optomechanical entanglement in a dissipative optomechanical system with a mechanical parametric drive, *Phys. Rev. A* **98**, 063843 (2018).
- [57] Y.-F. Jiao, S.-D. Zhang, Y.-L. Zhang, A. Miranowicz, L.-M. Kuang, and H. Jing, Nonreciprocal Optomechanical Entanglement against Backscattering Losses, *Phys. Rev. Lett.* **125**, 143605 (2020).
- [58] Y.-F. Jiao, J.-X. Liu, Y. Li, R. Yang, L.-M. Kuang, and H. Jing, Nonreciprocal Enhancement of Remote Entanglement between Nonidentical Mechanical Oscillators, *Phys. Rev. Applied* **18**, 064008 (2022).
- [59] Y.-Y. Liu, Z.-M. Zhang, J.-H. Liu, J.-D. Wang, and Y.-F. Yu, Nonreciprocal coupling induced entanglement enhancement in a double-cavity optomechanical system, *Chinese Phys. B* **31**, 094203 (2022).
- [60] X.-Y. Lü, Y. Wu, J. R. Johansson, H. Jing, J. Zhang, and F. Nori, Squeezed Optomechanics with Phase-Matched Amplification and Dissipation, *Phys. Rev. Lett.* **114**, 093602 (2015).
- [61] W. Qin, A. Miranowicz, P.-B. Li, X.-Y. Lü, J. Q. You, and F. Nori, Exponentially Enhanced Light-Matter Interaction, Cooperativities, and Steady-State Entanglement Using Parametric Amplification, *Phys. Rev. Lett.* **120**, 093601 (2018).
- [62] W. Qin, A. Miranowicz, H. Jing, and F. Nori, Generating Long-Lived Macroscopically Distinct Superposition States in Atomic Ensembles, *Phys. Rev. Lett.* **127**, 093602 (2021).
- [63] Y.-H. Chen, W. Qin, X. Wang, A. Miranowicz, and F. Nori, Shortcuts to Adiabaticity for the Quantum Rabi Model: Efficient Generation of Giant Entangled Cat States via Parametric Amplification, *Phys. Rev. Lett.* **126**, 023602 (2021).
- [64] W. Qin, A. Miranowicz, and F. Nori, Beating the 3 dB Limit for Intracavity Squeezing and Its Application to Nondemolition Qubit Readout, *Phys. Rev. Lett.* **129**, 123602 (2022).
- [65] L. Tang, J. Tang, M. Chen, F. Nori, M. Xiao, and K. Xia, Quantum Squeezing Induced Optical Nonreciprocity, *Phys. Rev. Lett.* **128**, 083604 (2022).
- [66] D.-Y. Wang, L.-L. Yan, S.-L. Su, C.-H. Bai, H.-F. Wang, and E. Liang, Squeezing-induced nonreciprocal photon blockade in an optomechanical microresonator, *Opt. Express* **31**, 22343 (2023).
- [67] C.-P. Shen, J.-Q. Chen, X.-F. Pan, Y.-M. Ren, X.-L. Dong, X.-L. Hei, Y.-F. Qiao, and P.-B. Li, Tunable nonreciprocal photon correlations induced by directional quantum squeezing, *Phys. Rev. A* **108**, 023716 (2023).
- [68] K.-W. Huang, Y. Wu, and L.-G. Si, Parametric-amplification-induced nonreciprocal magnon laser, *Opt. Lett.* **47**, 3311 (2022).
- [69] M.-A. Lemonde, N. Didier, and A. A. Clerk, Enhanced nonlinear interactions in quantum optomechanics via mechanical amplification, *Nat. Commun.* **7**, 11338 (2016).
- [70] P.-B. Li, Y. Zhou, W.-B. Gao, and F. Nori, Enhancing Spin-Phonon and Spin-Spin Interactions Using Linear Resources in a Hybrid Quantum System, *Phys. Rev. Lett.* **125**, 153602 (2020).
- [71] X.-L. Hei, P.-B. Li, X.-F. Pan, and F. Nori, Enhanced Tripartite Interactions in Spin-Magnon-Mechanical Hybrid Systems, *Phys. Rev. Lett.* **130**, 073602 (2023).
- [72] X.-Y. Lü, L.-L. Zheng, G.-L. Zhu, and Y. Wu, Single-Photon-Triggered Quantum Phase Transition, *Phys. Rev. Applied* **9**, 064006 (2018).
- [73] G.-L. Zhu, X.-Y. Lü, L.-L. Zheng, Z.-M. Zhan, F. Nori, and Y. Wu, Single-photon-triggered quantum chaos, *Phys. Rev. A* **100**, 023825 (2019).
- [74] Z. Zhang, L. Shao, W. Lu, Y. Su, Y.-P. Wang, J. Liu, and X. Wang, Single-photon-triggered spin squeezing with decoherence reduction in optomechanics via phase matching, *Phys. Rev. A* **104**, 053517 (2021).
- [75] Y. Wang, J.-L. Wu, J.-X. Han, Y. Xia, Y.-Y. Jiang, and J. Song, Enhanced Phonon Blockade in a Weakly Coupled Hybrid System via Mechanical Parametric Amplification, *Phys. Rev. Applied* **17**, 024009 (2022).
- [76] Y. Wang, H.-L. Zhang, J.-L. Wu, J. Song, K. Yang, W. Qin, H. Jing, and L.-M. Kuang, Quantum parametric amplification of phonon-mediated magnon-spin interaction, *Sci. China Phys. Mech. Astron.* **66**, 110311 (2023).
- [77] T. Li, T.-Y. Bao, Y.-L. Zhang, C.-L. Zou, X.-B. Zou, and G.-C. Guo, Long-distance synchronization of unidirectionally cascaded optomechanical systems, *Opt. Express* **24**, 12336 (2016).
- [78] J. Sheng, X. Wei, C. Yang, and H. Wu, Self-Organized Synchronization of Phonon Lasers, *Phys. Rev. Lett.* **124**, 053604 (2020).
- [79] C.-L. Zhu, Y.-L. Liu, L. Yang, Y.-X. Liu, and J. Zhang, Synchronization in PT-symmetric optomechanical resonators, *Photon. Res.* **9**, 2152 (2021).

- [80] X. Ren, J. Pan, M. Yan, J. Sheng, C. Yang, Q. Zhang, H. Ma, Z. Wen, K. Huang, H. Wu, and H. Zeng, Dual-comb optomechanical spectroscopy, *Nat. Commun.* **14**, 5037 (2023).
- [81] K. Stannigel, P. Komar, S. J. M. Habraken, S. D. Bennett, M. D. Lukin, P. Zoller, and P. Rabl, Optomechanical Quantum Information Processing with Photons and Phonons, *Phys. Rev. Lett.* **109**, 013603 (2012).
- [82] G. Adesso, A. Serafini, and F. Illuminati, Extremal entanglement and mixedness in continuous variable systems, *Phys. Rev. A* **70**, 022318 (2004).
- [83] R. Simon, Peres-Horodecki Separability Criterion for Continuous Variable Systems, *Phys. Rev. Lett.* **84**, 2726 (2000).
- [84] A. W. Bruch, X. Liu, J. B. Surya, C.-L. Zou, and H. X. Tang, On-chip $\chi^{(2)}$ microring optical parametric oscillator, *Optica* **6**, 1361 (2019).
- [85] P. Liu, H. Wen, L. Ren, L. Shi, and X. Zhang, $\chi^{(2)}$ nonlinear photonics in integrated microresonators, *Front. Optoelectron.* **16**, 18 (2023).
- [86] J. Huang, D.-G. Lai, and J.-Q. Liao, Controllable generation of mechanical quadrature squeezing via dark-mode engineering in cavity optomechanics, *Phys. Rev. A* **108**, 013516 (2023).
- [87] B. Li, W. Qin, Y.-F. Jiao, C.-L. Zhai, X.-W. Xu, L.-M. Kuang, and H. Jing, Optomechanical Schrödinger cat states in a cavity Bose-Einstein condensate, *Fundamental Research* **3**, 15 (2023).

Supporting Information for “Tripartite quantum entanglement with squeezed optomechanics”

Ya-Feng Jiao,^{1,2} Yun-Lan Zuo,³ Yan Wang,^{1,2} Wangjun Lu,⁴ Jie-Qiao Liao,³ Le-Man Kuang,^{2,3,*} and Hui Jing^{2,3,†}

¹*School of Electronics and Information, Zhengzhou University of Light Industry, Zhengzhou 450001, China*

²*Academy for Quantum Science and Technology, Zhengzhou University of Light Industry, Zhengzhou 450002, China*

³*Key Laboratory of Low-Dimensional Quantum Structures and Quantum Control of Ministry of Education, Department of Physics and Synergetic Innovation Center for Quantum Effects and Applications, Hunan Normal University, Changsha 410081, China*

⁴*Institute of Engineering Education and Engineering Culture Innovation and Department of Maths and Physics, Hunan Institute of Engineering, Xiangtan 411104, China*

* lmkuang@hunnu.edu.cn

† jinghui73@foxmail.com

S1. DERIVATION OF THE EFFECTIVE HAMILTONIAN AND MASTER EQUATION

The Hamiltonian of the cavity mode H_c in Eq. (1) includes two quadratic terms describing the nonlinear optical interaction induced by OPA. To introduce the squeezed cavity mode for H_c , one can perform a unitary Bogoliubov transformation with $S(\eta_d) = \exp[(-\eta_d \hat{c}^{\dagger 2} + \eta_d^* \hat{c}^2)/2]$, where $\eta_d = r_d \exp(-i\theta_d)$ is a complex number with a squeezing strength r_d and a squeezing reference angle θ_d . By employing the Bogoliubov transformation, the system Hamiltonian in Eq. (1) becomes

$$\begin{aligned}
 \tilde{H} &= S^\dagger(\eta_d) H S(\eta_d) \\
 &= \omega_{m,1} \hat{b}_1^\dagger \hat{b}_1 + \omega_{m,2} \hat{b}_2^\dagger \hat{b}_2 + \chi (e^{-i\varphi} \hat{b}_1^\dagger \hat{b}_2 + e^{i\varphi} \hat{b}_2^\dagger \hat{b}_1) + F_1 (\hat{b}_1^\dagger + \hat{b}_1) + F_2 (\hat{b}_2^\dagger + \hat{b}_2) \\
 &\quad + [\Delta_c \cosh(2r_d) - 2\Xi_d \sinh(2r_d)] \hat{c}_s^\dagger \hat{c}_s \\
 &\quad + \left[\Xi_d \cosh(2r_d) - \frac{\Delta_c}{2} \sinh(2r_d) \right] e^{-i\theta_d} \hat{c}_s^{\dagger 2} \\
 &\quad + \left[\Xi_d \cosh(2r_d) - \frac{\Delta_c}{2} \sinh(2r_d) \right] e^{i\theta_d} \hat{c}_s^2 \\
 &\quad - g_1 \left[\cosh(2r_d) \hat{c}_s^\dagger \hat{c}_s - \frac{1}{2} \sinh(2r_d) (e^{-i\theta_d} \hat{c}_s^{\dagger 2} + e^{i\theta_d} \hat{c}_s^2) + \sinh^2(r_d) \right] (\hat{b}_1^\dagger + \hat{b}_1) \\
 &\quad - g_2 \left[\cosh(2r_d) \hat{c}_s^\dagger \hat{c}_s - \frac{1}{2} \sinh(2r_d) (e^{-i\theta_d} \hat{c}_s^{\dagger 2} + e^{i\theta_d} \hat{c}_s^2) + \sinh^2(r_d) \right] (\hat{b}_2^\dagger + \hat{b}_2) \\
 &\quad + i\varepsilon_d \cosh(r_d) (\hat{c}_s^\dagger - \hat{c}_s) + i\varepsilon_d \sinh(r_d) (e^{-i\theta_d} \hat{c}_s^\dagger - e^{i\theta_d} \hat{c}_s) \\
 &\quad + \Delta_c \sinh^2(r_d) - \Xi_d \sinh(2r_d). \tag{S1.1}
 \end{aligned}$$

To diagonalize the Hamiltonian of the cavity mode and cancel the force induced by the parametric amplification, we set

$$\begin{aligned}
 \Xi_d \cosh(2r_d) - \frac{\Delta_c}{2} \sinh(2r_d) &= 0, \\
 F_j - g_j \sinh^2(r_d) &= 0, \tag{S1.2}
 \end{aligned}$$

and then one can obtain $r_d = (1/4) \ln[(\Delta_c + 2\Xi_d)/(\Delta_c - 2\Xi_d)]$ and $F_j = g_j \sinh^2(r_d)$. As a result, the effective Hamiltonian of the system can be obtained as

$$\begin{aligned}
 \tilde{H} &= \omega_s \hat{c}_s^\dagger \hat{c}_s + \omega_{m,1} \hat{b}_1^\dagger \hat{b}_1 + \omega_{m,2} \hat{b}_2^\dagger \hat{b}_2 + \chi (e^{-i\varphi} \hat{b}_1^\dagger \hat{b}_2 + e^{i\varphi} \hat{b}_2^\dagger \hat{b}_1) \\
 &\quad - \zeta_{s,1} \hat{c}_s^\dagger \hat{c}_s (\hat{b}_1^\dagger + \hat{b}_1) + \frac{\zeta_{p,1}}{2} (e^{-i\theta_d} \hat{c}_s^{\dagger 2} + e^{i\theta_d} \hat{c}_s^2) (\hat{b}_1^\dagger + \hat{b}_1) \\
 &\quad - \zeta_{s,2} \hat{c}_s^\dagger \hat{c}_s (\hat{b}_2^\dagger + \hat{b}_2) + \frac{\zeta_{p,2}}{2} (e^{-i\theta_d} \hat{c}_s^{\dagger 2} + e^{i\theta_d} \hat{c}_s^2) (\hat{b}_2^\dagger + \hat{b}_2) \\
 &\quad + i\varepsilon_d \cosh(r_d) (\hat{c}_s^\dagger - \hat{c}_s) + i\varepsilon_d \sinh(r_d) (e^{-i\theta_d} \hat{c}_s^\dagger - e^{i\theta_d} \hat{c}_s), \tag{S1.3}
 \end{aligned}$$

where

$$\begin{aligned}
\omega_s &= \Delta_c \cosh(2r_d) - 2\Xi_d \sinh(2r_d) = (\Delta_c - 2\Xi_d) \exp(2r_d), \\
\zeta_{s,j} &= g_j \cosh(2r_d) = \frac{g_j \Delta_c}{\sqrt{\Delta_c^2 - 4\Xi_d^2}}, \\
\zeta_{p,j} &= g_j \sinh(2r_d) = \frac{2g_j G}{\sqrt{\Delta_c^2 - 4\Xi_d^2}}, \\
C &= \Delta_c \sinh^2(r_d) - G \sinh(2r_d).
\end{aligned} \tag{S1.4}$$

Correspondingly, the Lindblad operators under the Bogoliubov transformation becomes

$$\begin{aligned}
& S^\dagger(\eta_d) \mathcal{D}[\hat{c}] \rho S(\eta_d) \\
&= 2 \cosh^2(r_d) \hat{c}_s \tilde{\rho} \hat{c}_s^\dagger + 2 \sinh^2(r_d) \hat{c}_s^\dagger \tilde{\rho} \hat{c}_s - 2 \sinh(r_d) \cosh(r_d) (e^{-i\theta_d} \hat{c}_s^\dagger \tilde{\rho} \hat{c}_s^\dagger + e^{i\theta_d} \hat{c}_s \tilde{\rho} \hat{c}_s) \\
&\quad - [\cosh^2(r_d) \hat{c}_s^\dagger \hat{c}_s \tilde{\rho} + \sinh^2(r_d) \hat{c}_s \hat{c}_s^\dagger \tilde{\rho} - \sinh(r_d) \cosh(r_d) (e^{-i\theta_d} \hat{c}_s^\dagger \hat{c}_s^\dagger \tilde{\rho} + e^{i\theta_d} \hat{c}_s \hat{c}_s \tilde{\rho})] \\
&\quad - [\cosh^2(r_d) \tilde{\rho} \hat{c}_s^\dagger \hat{c}_s + \sinh^2(r_d) \tilde{\rho} \hat{c}_s \hat{c}_s^\dagger - \sinh(r_d) \cosh(r_d) (e^{-i\theta_d} \tilde{\rho} \hat{c}_s^\dagger \hat{c}_s^\dagger + e^{i\theta_d} \tilde{\rho} \hat{c}_s \hat{c}_s)], \\
& S^\dagger \mathcal{G}[\hat{c}] \rho S(\eta_d) \\
&= 2e^{-2i\theta_d} \sinh^2(r_d) \hat{c}_s^\dagger \tilde{\rho} \hat{c}_s^\dagger + 2 \cosh^2(r_d) \hat{c}_s \tilde{\rho} \hat{c}_s - 2e^{-i\theta_d} \sinh(r_d) \cosh(r_d) (\hat{c}_s^\dagger \tilde{\rho} \hat{c}_s + \hat{c}_s \tilde{\rho} \hat{c}_s^\dagger) \\
&\quad - [e^{-2i\theta_d} \sinh^2(r_d) \hat{c}_s^\dagger \hat{c}_s^\dagger \tilde{\rho} + \cosh^2(r_d) \hat{c}_s \hat{c}_s \tilde{\rho} - e^{-i\theta_d} \sinh(r_d) \cosh(r_d) (\hat{c}_s^\dagger \hat{c}_s \tilde{\rho} + \hat{c}_s \hat{c}_s^\dagger \tilde{\rho})] \\
&\quad - [e^{-2i\theta_d} \sinh^2(r_d) \tilde{\rho} \hat{c}_s^\dagger \hat{c}_s^\dagger + \cosh^2(r_d) \tilde{\rho} \hat{c}_s \hat{c}_s - e^{-i\theta_d} \sinh(r_d) \cosh(r_d) (\tilde{\rho} \hat{c}_s^\dagger \hat{c}_s + \tilde{\rho} \hat{c}_s \hat{c}_s^\dagger)],
\end{aligned} \tag{S1.5}$$

yielding the effective master equation as

$$\begin{aligned}
\dot{\tilde{\rho}} &= S^\dagger(\eta_d) \dot{\rho} S(\eta_d) \\
&= i[\tilde{\rho}, \tilde{H}] + \frac{\kappa}{2} (N_s + 1) \mathcal{D}[\hat{c}_s] \tilde{\rho} + \frac{\kappa}{2} N_s \mathcal{D}[\hat{c}_s^\dagger] \tilde{\rho} - \frac{\kappa}{2} M_s \mathcal{G}[\hat{c}_s] \tilde{\rho} - \frac{\kappa}{2} M_s^* \mathcal{G}[\hat{c}_s^\dagger] \tilde{\rho} \\
&\quad + \sum_{j=1,2} \frac{\gamma_{m,j}}{2} (\bar{n}_{m,j} + 1) \mathcal{D}[\hat{b}_j] \tilde{\rho} + \frac{\gamma_{m,j}}{2} \bar{n}_{m,j} \mathcal{D}[\hat{b}_j^\dagger] \tilde{\rho},
\end{aligned} \tag{S1.6}$$

where

$$\begin{aligned}
N_s &= \sinh^2(r_d) \cosh^2(r_e) + \cosh^2(r_d) \sinh^2(r_e) + \frac{1}{2} \cos(\theta_e - \theta_d) \sinh(2r_d) \sinh(2r_e), \\
M_s &= e^{i\theta_d} [\cosh(r_d) \cosh(r_e) + e^{-i(\theta_e - \theta_d)} \sinh(r_d) \sinh(r_e)] \times [\sinh(r_d) \cosh(r_e) + e^{i(\theta_e - \theta_d)} \cosh(r_d) \sinh(r_e)].
\end{aligned}$$

Here N_s and M_s denote the effective thermal noise and two-photon-correlation strength, respectively, which can be simplified in case of $r_d = r_e = r$, i.e.,

$$\begin{aligned}
N_s &= \frac{1}{2} \sinh^2(2r) [1 + \cos(\theta_e - \theta_d)], \\
M_s &= \frac{1}{2} e^{i\theta_d} \sinh(2r) [1 + e^{i(\theta_e - \theta_d)}] [\cosh^2(r) + e^{-i(\theta_e - \theta_d)} \sinh^2(r)].
\end{aligned} \tag{S1.7}$$

S2. DERIVATION OF THE DYNAMICS OF QUANTUM CORRELATION FUNCTION

Equations (19) and (20) indicate that the matrix elements satisfy the relation of $V_{kl} = V_{lk}$, and that they are related to the quantum correlation functions for the associated optical and mechanical modes in terms of bosonic operators, i.e.,

$$\begin{aligned}
V_{11} &= \text{Re}[x_7] + x_1 + \frac{1}{2}, \quad V_{22} = -\text{Re}[x_7] + x_1 + \frac{1}{2}, \quad V_{33} = \text{Re}[x_9] + x_3 + \frac{1}{2}, \\
V_{44} &= -\text{Re}[x_9] + x_3 + \frac{1}{2}, \quad V_{55} = \text{Re}[x_{11}] + x_5 + \frac{1}{2}, \quad V_{66} = -\text{Re}[x_{11}] + x_5 + \frac{1}{2}, \\
V_{12} &= \text{Im}[x_7], \quad V_{34} = \text{Im}[x_9], \quad V_{56} = \text{Im}[x_{11}], \\
V_{13} &= \text{Re}[x_{13}] + \text{Re}[x_{15}], \quad V_{14} = \text{Im}[x_{13}] - \text{Im}[x_{15}], \quad V_{15} = \text{Re}[x_{17}] + \text{Re}[x_{19}], \\
V_{16} &= \text{Im}[x_{17}] - \text{Im}[x_{19}], \quad V_{23} = \text{Im}[x_{13}] + \text{Im}[x_{15}], \quad V_{24} = -\text{Re}[x_{13}] + \text{Re}[x_{15}], \\
V_{25} &= \text{Im}[x_{17}] + \text{Im}[x_{19}], \quad V_{26} = -\text{Re}[x_{17}] + \text{Re}[x_{19}], \quad V_{35} = \text{Re}[x_{21}] + \text{Re}[x_{23}], \\
V_{36} &= \text{Im}[x_{21}] - \text{Im}[x_{23}], \quad V_{45} = \text{Im}[x_{21}] + \text{Im}[x_{23}], \quad V_{46} = -\text{Re}[x_{21}] + \text{Re}[x_{23}],
\end{aligned} \tag{S2.8}$$

with

$$\begin{aligned}
x_1 &= \langle \hat{c}_s^\dagger \hat{c}_s \rangle, \quad x_2 = \langle \hat{c}_s^\dagger \hat{c}_s^\dagger \rangle, \quad x_3 = \langle \hat{b}_1^\dagger \hat{b}_1 \rangle, \quad x_4 = \langle \hat{b}_1^\dagger \hat{b}_1^\dagger \rangle, \quad x_5 = \langle \hat{b}_2^\dagger \hat{b}_2 \rangle, \quad x_6 = \langle \hat{b}_2^\dagger \hat{b}_2^\dagger \rangle, \\
x_7 &= \langle \hat{c}_s \hat{c}_s \rangle, \quad x_8 = \langle \hat{c}_s \hat{c}_s^\dagger \rangle, \quad x_9 = \langle \hat{b}_1 \hat{b}_1 \rangle, \quad x_{10} = \langle \hat{b}_1^\dagger \hat{b}_1^\dagger \rangle, \quad x_{11} = \langle \hat{b}_2 \hat{b}_2 \rangle, \quad x_{12} = \langle \hat{b}_2^\dagger \hat{b}_2^\dagger \rangle, \\
x_{13} &= \langle \hat{c}_s \hat{b}_1 \rangle, \quad x_{14} = \langle \hat{c}_s^\dagger \hat{b}_1^\dagger \rangle, \quad x_{15} = \langle \hat{c}_s \hat{b}_1^\dagger \rangle, \quad x_{16} = \langle \hat{c}_s^\dagger \hat{b}_1 \rangle, \quad x_{17} = \langle \hat{c}_s \hat{b}_2 \rangle, \quad x_{18} = \langle \hat{c}_s^\dagger \hat{b}_2^\dagger \rangle, \\
x_{19} &= \langle \hat{c}_s \hat{b}_2^\dagger \rangle, \quad x_{20} = \langle \hat{c}_s^\dagger \hat{b}_2 \rangle, \quad x_{21} = \langle \hat{b}_1 \hat{b}_2 \rangle, \quad x_{22} = \langle \hat{b}_1^\dagger \hat{b}_2^\dagger \rangle, \quad x_{23} = \langle \hat{b}_1 \hat{b}_2^\dagger \rangle, \quad x_{24} = \langle \hat{b}_1^\dagger \hat{b}_2 \rangle.
\end{aligned} \tag{S2.9}$$

By employing the linearized effective master equation (14), the equation of motion of the quantum correlation function in the vector X can be derived as

$$\begin{aligned}
\frac{d}{dt} \langle \hat{c}_s^\dagger \hat{c}_s \rangle &= -\kappa \langle \hat{c}_s^\dagger \hat{c}_s \rangle + i\Lambda_1 \langle \hat{c}_s^\dagger \hat{b}_1^\dagger \rangle + i\Lambda_1 \langle \hat{c}_s^\dagger \hat{b}_1 \rangle - i\Lambda_1^* \langle \hat{c}_s \hat{b}_1^\dagger \rangle - i\Lambda_1^* \langle \hat{c}_s \hat{b}_1 \rangle + i\Lambda_2 \langle \hat{c}_s^\dagger \hat{b}_2^\dagger \rangle \\
&\quad + i\Lambda_2 \langle \hat{c}_s^\dagger \hat{b}_2 \rangle - i\Lambda_2^* \langle \hat{c}_s \hat{b}_2^\dagger \rangle - i\Lambda_2^* \langle \hat{c}_s \hat{b}_2 \rangle + \kappa N_s,
\end{aligned} \tag{S2.10}$$

$$\begin{aligned}
\frac{d}{dt} \langle \hat{c}_s \hat{c}_s^\dagger \rangle &= -\kappa \langle \hat{c}_s \hat{c}_s^\dagger \rangle - i\Lambda_1^* \langle \hat{c}_s \hat{b}_1 \rangle - i\Lambda_1^* \langle \hat{c}_s \hat{b}_1^\dagger \rangle + i\Lambda_1 \langle \hat{c}_s^\dagger \hat{b}_1 \rangle + i\Lambda_1 \langle \hat{c}_s^\dagger \hat{b}_1^\dagger \rangle - i\Lambda_2^* \langle \hat{c}_s \hat{b}_2 \rangle \\
&\quad - i\Lambda_2^* \langle \hat{c}_s \hat{b}_2^\dagger \rangle + i\Lambda_2 \langle \hat{c}_s^\dagger \hat{b}_2 \rangle + i\Lambda_2 \langle \hat{c}_s^\dagger \hat{b}_2^\dagger \rangle + \kappa(N_s + 1),
\end{aligned} \tag{S2.11}$$

$$\begin{aligned}
\frac{d}{dt} \langle \hat{b}_1^\dagger \hat{b}_1 \rangle &= -\gamma_{m,1} \langle \hat{b}_1^\dagger \hat{b}_1 \rangle + i\Lambda_1 \langle \hat{c}_s^\dagger \hat{b}_1^\dagger \rangle + i\Lambda_1^* \langle \hat{c}_s \hat{b}_1^\dagger \rangle - i\Lambda_1 \langle \hat{c}_s^\dagger \hat{b}_1 \rangle - i\Lambda_1^* \langle \hat{c}_s \hat{b}_1 \rangle - i\chi e^{-i\varphi} \langle \hat{b}_1^\dagger \hat{b}_2 \rangle \\
&\quad + i\chi e^{i\varphi} \langle \hat{b}_2^\dagger \hat{b}_1 \rangle + \gamma_{m,1} \bar{n}_{m,1},
\end{aligned} \tag{S2.12}$$

$$\begin{aligned}
\frac{d}{dt} \langle \hat{b}_1 \hat{b}_1^\dagger \rangle &= -\gamma_{m,1} \langle \hat{b}_1 \hat{b}_1^\dagger \rangle - i\Lambda_1^* \langle \hat{c}_s \hat{b}_1 \rangle - i\Lambda_1 \langle \hat{c}_s^\dagger \hat{b}_1 \rangle + i\Lambda_1^* \langle \hat{c}_s \hat{b}_1^\dagger \rangle + i\Lambda_1 \langle \hat{c}_s^\dagger \hat{b}_1^\dagger \rangle + i\chi e^{i\varphi} \langle \hat{b}_1 \hat{b}_2^\dagger \rangle \\
&\quad - i\chi e^{-i\varphi} \langle \hat{b}_2 \hat{b}_1^\dagger \rangle + \gamma_{m,1}(\bar{n}_{m,1} + 1),
\end{aligned} \tag{S2.13}$$

$$\begin{aligned}
\frac{d}{dt} \langle \hat{b}_2^\dagger \hat{b}_2 \rangle &= -\gamma_{m,2} \langle \hat{b}_2^\dagger \hat{b}_2 \rangle + i\Lambda_2 \langle \hat{c}_s^\dagger \hat{b}_2^\dagger \rangle + i\Lambda_2^* \langle \hat{c}_s \hat{b}_2^\dagger \rangle - i\Lambda_2 \langle \hat{c}_s^\dagger \hat{b}_2 \rangle - i\Lambda_2^* \langle \hat{c}_s \hat{b}_2 \rangle + i\chi e^{-i\varphi} \langle \hat{b}_1^\dagger \hat{b}_2 \rangle \\
&\quad - i\chi e^{i\varphi} \langle \hat{b}_2^\dagger \hat{b}_1 \rangle + \gamma_{m,2} \bar{n}_{m,2},
\end{aligned} \tag{S2.14}$$

$$\begin{aligned}
\frac{d}{dt} \langle \hat{b}_2 \hat{b}_2^\dagger \rangle &= -\gamma_{m,2} \langle \hat{b}_2 \hat{b}_2^\dagger \rangle - i\Lambda_2^* \langle \hat{c}_s \hat{b}_2 \rangle - i\Lambda_2 \langle \hat{c}_s^\dagger \hat{b}_2 \rangle + i\Lambda_2^* \langle \hat{c}_s \hat{b}_2^\dagger \rangle + i\Lambda_2 \langle \hat{c}_s^\dagger \hat{b}_2^\dagger \rangle - i\chi e^{i\varphi} \langle \hat{b}_1 \hat{b}_2^\dagger \rangle \\
&\quad + i\chi e^{-i\varphi} \langle \hat{b}_2 \hat{b}_1^\dagger \rangle + \gamma_{m,2}(\bar{n}_{m,2} + 1),
\end{aligned} \tag{S2.15}$$

$$\frac{d}{dt} \langle \hat{c}_s \hat{c}_s \rangle = -(2i\Delta_s + \kappa) \langle \hat{c}_s \hat{c}_s \rangle + 2i\Lambda_1 \langle \hat{c}_s \hat{b}_1^\dagger \rangle + 2i\Lambda_1 \langle \hat{c}_s \hat{b}_1 \rangle + 2i\Lambda_2 \langle \hat{c}_s \hat{b}_2^\dagger \rangle + 2i\Lambda_2 \langle \hat{c}_s \hat{b}_2 \rangle + \kappa M_s^*, \quad (\text{S2.16})$$

$$\frac{d}{dt} \langle \hat{c}_s^\dagger \hat{c}_s^\dagger \rangle = (2i\Delta_s - \kappa) \langle \hat{c}_s^\dagger \hat{c}_s^\dagger \rangle - 2i\Lambda_1^* \langle \hat{c}_s^\dagger \hat{b}_1 \rangle - 2i\Lambda_1^* \langle \hat{c}_s^\dagger \hat{b}_1^\dagger \rangle - 2i\Lambda_2^* \langle \hat{c}_s^\dagger \hat{b}_2 \rangle - 2i\Lambda_2^* \langle \hat{c}_s^\dagger \hat{b}_2^\dagger \rangle + \kappa M_s, \quad (\text{S2.17})$$

$$\frac{d}{dt} \langle \hat{b}_1 \hat{b}_1 \rangle = -(2i\omega_{m,1} + \gamma_{m,1}) \langle \hat{b}_1 \hat{b}_1 \rangle + 2i\Lambda_1 \langle \hat{c}_s^\dagger \hat{b}_1 \rangle + 2i\Lambda_1^* \langle \hat{c}_s \hat{b}_1 \rangle - 2i\chi e^{-i\varphi} \langle \hat{b}_1 \hat{b}_2 \rangle, \quad (\text{S2.18})$$

$$\frac{d}{dt} \langle \hat{b}_1^\dagger \hat{b}_1^\dagger \rangle = (2i\omega_{m,1} - \gamma_{m,1}) \langle \hat{b}_1^\dagger \hat{b}_1^\dagger \rangle - 2i\Lambda_1^* \langle \hat{c}_s \hat{b}_1^\dagger \rangle - 2i\Lambda_1 \langle \hat{c}_s^\dagger \hat{b}_1^\dagger \rangle + 2i\chi e^{i\varphi} \langle \hat{b}_1^\dagger \hat{b}_2^\dagger \rangle, \quad (\text{S2.19})$$

$$\frac{d}{dt} \langle \hat{b}_2 \hat{b}_2 \rangle = -(2i\omega_{m,2} + \gamma_{m,2}) \langle \hat{b}_2 \hat{b}_2 \rangle + 2i\Lambda_2 \langle \hat{c}_s^\dagger \hat{b}_2 \rangle + 2i\Lambda_2^* \langle \hat{c}_s \hat{b}_2 \rangle - 2i\chi e^{i\varphi} \langle \hat{b}_1 \hat{b}_2 \rangle, \quad (\text{S2.20})$$

$$\frac{d}{dt} \langle \hat{b}_2^\dagger \hat{b}_2^\dagger \rangle = (2i\omega_{m,2} - \gamma_{m,2}) \langle \hat{b}_2^\dagger \hat{b}_2^\dagger \rangle - 2i\Lambda_2^* \langle \hat{c}_s \hat{b}_2^\dagger \rangle - 2i\Lambda_2 \langle \hat{c}_s^\dagger \hat{b}_2^\dagger \rangle + 2i\chi e^{-i\varphi} \langle \hat{b}_1^\dagger \hat{b}_2^\dagger \rangle, \quad (\text{S2.21})$$

$$\begin{aligned} \frac{d}{dt} \langle \hat{c}_s \hat{b}_1 \rangle &= -[(i\Delta_s + \omega_{m,1}) + \frac{\kappa + \gamma_{m,1}}{2}] \langle \hat{c}_s \hat{b}_1 \rangle + i\Lambda_1 \langle \hat{c}_s^\dagger \hat{c}_s \rangle + i\Lambda_1 \langle \hat{b}_1 \hat{b}_1^\dagger \rangle + i\Lambda_1 \langle \hat{b}_1 \hat{b}_1 \rangle \\ &\quad + i\Lambda_1^* \langle \hat{c}_s \hat{c}_s \rangle + i\Lambda_2 \langle \hat{b}_1 \hat{b}_2^\dagger \rangle + i\Lambda_2 \langle \hat{b}_1 \hat{b}_2 \rangle - i\chi e^{-i\varphi} \langle \hat{c}_s \hat{b}_2 \rangle, \end{aligned} \quad (\text{S2.22})$$

$$\begin{aligned} \frac{d}{dt} \langle \hat{c}_s^\dagger \hat{b}_1^\dagger \rangle &= [(i\Delta_s + \omega_{m,1}) - \frac{\kappa + \gamma_{m,1}}{2}] \langle \hat{c}_s^\dagger \hat{b}_1^\dagger \rangle - i\Lambda_1^* \langle \hat{c}_s \hat{c}_s^\dagger \rangle - i\Lambda_1^* \langle \hat{b}_1 \hat{b}_1 \rangle - i\Lambda_1^* \langle \hat{b}_1^\dagger \hat{b}_1^\dagger \rangle \\ &\quad - i\Lambda_1 \langle \hat{c}_s^\dagger \hat{c}_s \rangle - i\Lambda_2^* \langle \hat{b}_1^\dagger \hat{b}_2 \rangle - i\Lambda_2^* \langle \hat{b}_1^\dagger \hat{b}_2^\dagger \rangle + i\chi e^{i\varphi} \langle \hat{c}_s^\dagger \hat{b}_2^\dagger \rangle, \end{aligned} \quad (\text{S2.23})$$

$$\begin{aligned} \frac{d}{dt} \langle \hat{c}_s \hat{b}_1^\dagger \rangle &= -[i(\Delta_s - \omega_{m,1}) + \frac{\kappa + \gamma_{m,1}}{2}] \langle \hat{c}_s \hat{b}_1^\dagger \rangle + i\Lambda_1 \langle \hat{b}_1^\dagger \hat{b}_1^\dagger \rangle - i\Lambda_1 \langle \hat{c}_s^\dagger \hat{c}_s \rangle + i\Lambda_1 \langle \hat{b}_1^\dagger \hat{b}_1 \rangle \\ &\quad - i\Lambda_1^* \langle \hat{c}_s \hat{c}_s \rangle + i\Lambda_2 \langle \hat{b}_1^\dagger \hat{b}_2^\dagger \rangle + i\Lambda_2 \langle \hat{b}_1^\dagger \hat{b}_2 \rangle + i\chi e^{i\varphi} \langle \hat{c}_s \hat{b}_2^\dagger \rangle, \end{aligned} \quad (\text{S2.24})$$

$$\begin{aligned} \frac{d}{dt} \langle \hat{c}_s^\dagger \hat{b}_1 \rangle &= [i(\Delta_s - \omega_{m,1}) - \frac{\kappa + \gamma_{m,1}}{2}] \langle \hat{c}_s^\dagger \hat{b}_1 \rangle - i\Lambda_1^* \langle \hat{b}_1 \hat{b}_1 \rangle + i\Lambda_1^* \langle \hat{c}_s \hat{c}_s^\dagger \rangle - i\Lambda_1^* \langle \hat{b}_1 \hat{b}_1^\dagger \rangle \\ &\quad + i\Lambda_1 \langle \hat{c}_s^\dagger \hat{c}_s \rangle - i\Lambda_2^* \langle \hat{b}_1 \hat{b}_2 \rangle - i\Lambda_2^* \langle \hat{b}_1 \hat{b}_2^\dagger \rangle - i\chi e^{-i\varphi} \langle \hat{c}_s^\dagger \hat{b}_2 \rangle, \end{aligned} \quad (\text{S2.25})$$

$$\begin{aligned} \frac{d}{dt} \langle \hat{c}_s \hat{b}_2 \rangle &= -[i(\Delta_s + \omega_{m,2}) + \frac{\kappa + \gamma_{m,2}}{2}] \langle \hat{c}_s \hat{b}_2 \rangle + i\Lambda_2 \langle \hat{c}_s^\dagger \hat{c}_s \rangle + i\Lambda_2 \langle \hat{b}_2 \hat{b}_2^\dagger \rangle + i\Lambda_2 \langle \hat{b}_2 \hat{b}_2 \rangle \\ &\quad + i\Lambda_2^* \langle \hat{c}_s \hat{c}_s \rangle + i\Lambda_1 \langle \hat{b}_1^\dagger \hat{b}_2 \rangle + i\Lambda_1 \langle \hat{b}_1 \hat{b}_2 \rangle - i\chi e^{i\varphi} \langle \hat{c}_s \hat{b}_1 \rangle, \end{aligned} \quad (\text{S2.26})$$

$$\begin{aligned} \frac{d}{dt} \langle \hat{c}_s^\dagger \hat{b}_2^\dagger \rangle &= [i(\Delta_s + \omega_{m,2}) - \frac{\kappa + \gamma_{m,2}}{2}] \langle \hat{c}_s^\dagger \hat{b}_2^\dagger \rangle - i\Lambda_2^* \langle \hat{c}_s \hat{c}_s^\dagger \rangle - i\Lambda_2^* \langle \hat{b}_2 \hat{b}_2 \rangle - i\Lambda_2^* \langle \hat{b}_2^\dagger \hat{b}_2^\dagger \rangle \\ &\quad - i\Lambda_2 \langle \hat{c}_s^\dagger \hat{c}_s \rangle - i\Lambda_1^* \langle \hat{b}_1 \hat{b}_2^\dagger \rangle - i\Lambda_1^* \langle \hat{b}_1^\dagger \hat{b}_2^\dagger \rangle + i\chi e^{-i\varphi} \langle \hat{c}_s^\dagger \hat{b}_1^\dagger \rangle, \end{aligned} \quad (\text{S2.27})$$

$$\begin{aligned} \frac{d}{dt} \langle \hat{c}_s \hat{b}_2^\dagger \rangle &= -[i(\Delta_s - \omega_{m,2}) + \frac{\kappa + \gamma_{m,2}}{2}] \langle \hat{c}_s \hat{b}_2^\dagger \rangle + i\Lambda_2 \langle \hat{b}_2^\dagger \hat{b}_2^\dagger \rangle - i\Lambda_2 \langle \hat{c}_s^\dagger \hat{c}_s \rangle + i\Lambda_2 \langle \hat{b}_2^\dagger \hat{b}_2 \rangle \\ &\quad - i\Lambda_2^* \langle \hat{c}_s \hat{c}_s \rangle + i\Lambda_1 \langle \hat{b}_1^\dagger \hat{b}_2^\dagger \rangle + i\Lambda_1 \langle \hat{b}_1 \hat{b}_2 \rangle + i\chi e^{-i\varphi} \langle \hat{c}_s \hat{b}_1^\dagger \rangle, \end{aligned} \quad (\text{S2.28})$$

$$\begin{aligned} \frac{d}{dt} \langle \hat{c}_s^\dagger \hat{b}_2 \rangle = & [i(\Delta_s - \omega_{m,2}) - \frac{\kappa + \gamma_{m,2}}{2}] \langle \hat{c}_s^\dagger \hat{b}_2 \rangle - i\Lambda_2^* \langle \hat{b}_2 \hat{b}_2 \rangle + i\Lambda_2^* \langle \hat{c}_s \hat{c}_s^\dagger \rangle - i\Lambda_2^* \langle \hat{b}_2 \hat{b}_2^\dagger \rangle \\ & + i\Lambda_2 \langle \hat{c}_s^\dagger \hat{c}_s^\dagger \rangle - i\Lambda_1^* \langle \hat{b}_1 \hat{b}_2 \rangle - i\Lambda_1^* \langle \hat{b}_1^\dagger \hat{b}_2 \rangle - i\chi e^{i\varphi} \langle \hat{c}_s^\dagger \hat{b}_1 \rangle, \end{aligned} \quad (\text{S2.29})$$

$$\begin{aligned} \frac{d}{dt} \langle \hat{b}_1 \hat{b}_2 \rangle = & - [i(\omega_{m,1} + \omega_{m,2}) + \frac{\gamma_{m,1} + \gamma_{m,2}}{2}] \langle \hat{b}_1 \hat{b}_2 \rangle + i\Lambda_1 \langle \hat{c}_s^\dagger \hat{b}_2 \rangle + i\Lambda_1^* \langle \hat{c}_s \hat{b}_2 \rangle + i\Lambda_2 \langle \hat{c}_s^\dagger \hat{b}_1 \rangle \\ & + i\Lambda_2^* \langle \hat{c}_s \hat{b}_1 \rangle - i\chi e^{i\varphi} \langle \hat{b}_1 \hat{b}_1 \rangle - i\chi e^{-i\varphi} \langle \hat{b}_2 \hat{b}_2 \rangle, \end{aligned} \quad (\text{S2.30})$$

$$\begin{aligned} \frac{d}{dt} \langle \hat{b}_1^\dagger \hat{b}_2^\dagger \rangle = & [i(\omega_{m,1} + \omega_{m,2}) - \frac{\gamma_{m,1} + \gamma_{m,2}}{2}] \langle \hat{b}_1^\dagger \hat{b}_2^\dagger \rangle - i\Lambda_1^* \langle \hat{c}_s \hat{b}_2^\dagger \rangle - i\Lambda_1 \langle \hat{c}_s^\dagger \hat{b}_2^\dagger \rangle - i\Lambda_2^* \langle \hat{c}_s \hat{b}_1^\dagger \rangle \\ & - i\Lambda_2 \langle \hat{c}_s^\dagger \hat{b}_1^\dagger \rangle + i\chi e^{-i\varphi} \langle \hat{b}_1^\dagger \hat{b}_1^\dagger \rangle + i\chi e^{i\varphi} \langle \hat{b}_2^\dagger \hat{b}_2^\dagger \rangle, \end{aligned} \quad (\text{S2.31})$$

$$\begin{aligned} \frac{d}{dt} \langle \hat{b}_1 \hat{b}_2^\dagger \rangle = & - [i(\omega_{m,1} - \omega_{m,2}) + \frac{\gamma_{m,1} + \gamma_{m,2}}{2}] \langle \hat{b}_1 \hat{b}_2^\dagger \rangle + i\Lambda_1 \langle \hat{c}_s^\dagger \hat{b}_2^\dagger \rangle + i\Lambda_1^* \langle \hat{c}_s \hat{b}_2^\dagger \rangle - i\Lambda_2 \langle \hat{c}_s^\dagger \hat{b}_1 \rangle \\ & - i\Lambda_2^* \langle \hat{c}_s \hat{b}_1 \rangle + i\chi e^{-i\varphi} \langle \hat{b}_1 \hat{b}_1^\dagger \rangle - i\chi e^{-i\varphi} \langle \hat{b}_2 \hat{b}_2^\dagger \rangle, \end{aligned} \quad (\text{S2.32})$$

$$\begin{aligned} \frac{d}{dt} \langle \hat{b}_1^\dagger \hat{b}_2 \rangle = & [i(\omega_{m,1} - \omega_{m,2}) - \frac{\gamma_{m,1} + \gamma_{m,2}}{2}] \langle \hat{b}_1^\dagger \hat{b}_2 \rangle - i\Lambda_1^* \langle \hat{c}_s \hat{b}_2 \rangle - i\Lambda_1 \langle \hat{c}_s^\dagger \hat{b}_2 \rangle + i\Lambda_2^* \langle \hat{c}_s \hat{b}_1^\dagger \rangle \\ & + i\Lambda_2 \langle \hat{c}_s^\dagger \hat{b}_1^\dagger \rangle - i\chi e^{i\varphi} \langle \hat{b}_1^\dagger \hat{b}_1 \rangle + i\chi e^{i\varphi} \langle \hat{b}_2^\dagger \hat{b}_2 \rangle. \end{aligned} \quad (\text{S2.33})$$

Then, by rewriting the above time evolution equations in a matrix form with the vector X , one can obtain

$$\frac{d}{dt} X = M \cdot X + N, \quad (\text{S2.34})$$

$$\Omega_{8,\pm} = i(\omega_{m,1} + \omega_{m,2}) \pm \frac{\gamma_{m,1} + \gamma_{m,2}}{2}, \quad \Omega_{9,\pm} = i(\omega_{m,1} - \omega_{m,2}) \pm \frac{\gamma_{m,1} + \gamma_{m,2}}{2}. \quad (\text{S2.38})$$